LAPPEENRANTA-LAHTI UNIVERSITY OF TECHNOLOGY LUT
School of Energy systems
Electrical engineering

Max Lönnqvist

SHIP ENERGY EFFICIENCY ANALYSIS

Examiners: Professor Juha Pyrhönen
Associate professor Lasse Laurila

ABSTRAKT

Villmanstrand-Lahtis tekniska Universitet LUT
Skolan av Energi Systemen
Programmet inom elteknik

Max Lönnqvist

ENERGIEFFEKTIVITET ANALYS AV FARTYGAR

Magisters examen
2021
77 sidor, 31 bilder, 9 tabeller ja 4 bilagor
Inspektörer: Professor Juha Pyrhönen och tekn. dr Lasse Laurila

Sökord: Fartygets verkningsgrad, fartygets motstånd, effektkalkyl, axelgenerator, verkningsgrad.

Det globala importexport ekosystemet är beroende av väl upphållt och effektivt flotta av civila fartyg, på samma tid gemensamt nyttigt är att detta ekosystem funktionerar med det minsta kolfotavtrycket som möjligt. Målet för denna examenstext är att undersöka vilka faktorer omfattar effektiviteten av ett fartyg, och i vidare skede undersöka med att utnyttja operativdata från fartyget sig själva att hur dagens skepp kan byggas mera effektivare i framtiden. På grund av att alla maskiner är byggda för ett visst ändamål, är det viktigaste undersökningsproblemet att hur fartyg är opererade och byggda. Med den kända operationella hastighetsprofilen och information av fartygets konstruktion och komponenternas effektivitet, en uppskattning av fartygets bränsleförbrukning räknas med metoder av empirisk bakgrund. Operationella hastighetsprofilen samlas från Automatic Identification system data, och med empiriska metoderna konverteras till effekt.

Kalkylerna är repeterade med olika typ av maskinhelhet, målet med detta är att räkna ifall fartyget har speciell nytta av en axelgenerator eller diesel-elektrisk framdrivning, och hur ett visst fartyg av en viss typ och hastighetsprofil har nytta av dessa och hurdana skillnader i bränsleförbrukningar mellan fartyg typerna har med samma maskinhelhet. Den bästa möjliga slutsatsen för detta examenarbete är att räkna kvantitativa värden för hur mycket en axelgenerator eller diesel-elektrisk framdrivning sparar bränsle. Det moderna framdrivningssystemet, dess viktigaste komponenter och deras effektivitet på öppna marknader är undersökta med en litteratursundersökning. Den viktigaste källan för information är publikationer av tillverkare av komponenter till sjöfarten från de öppna-källorna. Detta kompletteras med frågeformulären till konsulter inom sjöfarts industrin och till dockar i Finland.

Studiet i korthet var en framgång, mål definierat i förhand var mötta. Studiet producerade en användbar kalkylmodell för alla att utnyttja. Största källorna for ineffektivitet hittades vara dieselmotorn och propellern. Effektiviteten av framdrivningen är i praktiken nära till värdet ett i både mekanisk och elektrisk framdrivning. Kalkylmodellen visade att en axelgenerator kan i rätta omgivningar spara 2 % i totala bränsleförbrukningen och diesel-elektriska framdrivningen till och med 5 %.

ABSTRACT

Lappeenranta-Lahti University of technology LUT
School of Energy Systems
Degree programme in Electrical engineering

Max Lönnqvist

SHIP ENERGY EFFICIENCY ANALYSIS

Master's thesis
2021
77 pages, 31 images, 9 tables ja 4 appendixes
Examiners: Professor Juha Pyrhönen and D.Sc Lasse Laurila.

Keywords: Ship efficiency, Ship resistance, power estimate, shaft generator, efficiency.

Export and import are heavily dependent on a well maintained and efficient fleet of ships, and a mutual interest within the mankind is to reduce the ecological footprint in all human activity, marine transport included. The aim of this thesis is to research the fundamental factors included in the efficiency of a ship and by operational data calculate how the ships of today could be built more fuel-efficient tomorrow. Since every ship is a machine built for a specific purpose, the main aim of this work is to study how ships are operated and how these ships are constructed. Together with operational speed profile and knowledge of ship construction and their efficiencies, an estimate of ship fuel consumption has been made using empirical calculation methods. The operational speed profile is based on Automatic Identification system data, from which the speed is converted into propulsion power.

The calculations are repeated with a different machinery design to find if a ship has significant advantage of a shaft generator or diesel electric propulsion, and if a ship type and speed profile have an impact on usefulness of a shaft generator or electric propulsion. Ultimate aim of this study is to gain a quantifiable number on how much a shaft generator or diesel electric propulsion saves fuel. The modern propulsion system, its main components and efficiencies are studied by a literature review of the systems existing in the open market. The main source of information are the open-source publications of manufacturers within the marine industry, and a series of questionnaires to naval consultant companies and shipyards in Finland.

The Study in a nutshell was successful, and the forehand placed goals were met. The study provided with a useful calculation model, which anyone can utilize. The biggest sources of inefficiencies onboard a ship are the diesel engine and the propeller. The efficiency of the power transmission is practically close to unity in both mechanical and electrical transmissions. The computations show that a use of a shaft generator can lower the total fuel consumption by up to 2 % and electric powertrain by up to 5 %.

ACKNOWLEDGEMENTS

I wish to thank both examiners for their positive corrections and guidance. I also like to thank Chief engineer Paul Salo, Masters of Science Markus Vauhkonen and Juhani Kankare and marine engineer Janne Saarinen for “the meat and potato” that came into this work.

Also, for the unsung heroes that were involved: thank you.

TABLE OF CONTENTS

Appendix 1 - Wageningen B polynomials

Appendix 2 - MATLAB propeller calculator

Appendix 3 - Ship resistance and power estimation calculator based on Holtrop-Mennen- and ITTC78-methods

Appendix 4 – Fuel consumption calculator

LIST OF SYMBOLS AND ABBREVIATIONS

AIS	Automatic Identification system	
BSFC	Best specific fuel consumption	
CFD	Computational fluid dynamics	
CII	carbon intensity index	
CPP	Controllable pitch propeller	
CRP	Contra-rotating propeller	
EEDI	Energy Efficiency Design Index	
EEXI	Energy Efficiency Existing Ship Index	
FPP	Fixed pitch propeller	
Kn	Knot, unit of speed used in marine traffic	1 Kn = 1.852 km/h
Nmi	Nautical mile, unit of distance in marine traffic	1 Nmi = 1.852 km
PTI/PTO	Power-take-in/Power-take-out	
RANS	Reynolds-averaged Navier-Stokes equations	
SFC	Specific fuel consumption	
TDC	Top-dead-center	

A_0	Actuator disc area	[m^2]
A_e/A_o	Propeller expanded area ratio	
C_b	The block coefficient	
C_f	Fuel specific energy	[MJ/kg]
C_p	Specific heat capacity under constant pressure	[kJ/kgK]
C_v	Specific heat capacity under constant volume	[kJ/kgK]
D_{pr}	Propeller diameter	[m]
D_{pi}	Piston bore	[m]
F_{pr}	Propeller thrust	[N]
f_c	Fuel consumption	[kg/s]
F_n	Normal force	[N]
F_p	Propeller thrust	[N]
F_t	Tangential force	[N]
H	Dynamic head	[Pa]
J	Advance ratio	

k	Hull form factor	
K_F	Thrust coefficient	
K_T	Torque coefficient	
n	Rotational speed	[1/s]
m_a	Mass of the air	[kg]
p	Pressure	[Pa]
p_i	Mean induced pressure	[Pa]
P_m	mechanical power in	[W]
P_D	Delivered propulsive power to the propeller	[W]
p_{et}	transverse pitch	[mm]
P/D	Pitch/diameter ratio of the propeller	
P_i	induced power	[W]
P_{VZP}	Load gear losses	[W]
Q	propeller torque	[Nm]
R_{AA}	air resistance	[N]
R_A	model-ship correlation resistance	[N]
R_{APP}	appendage resistance	[N]
R_B	bulbous resistance	[N]
R_F	frictional resistance	[N]
R_T	total resistance	[N]
R_{TH}	Thruster tunnel resistance	[N]
R_{TR}	transom resistance	[N]
R_W	wave resistance	[N]
S_p	Piston stroke in meters	[m]
t	thrust deduction factor	
v	velocity	[m/s]
v_a	speed of advance	[m/s]
v_s	speed of the vessel	[m/s]
v_p	pitch line velocity	[m/s]
v_g	sliding velocity	[m/s]
w_a	hull wake fraction	
Z_{pr}	number of blades on the propeller	
Z_c	number of engine cylinder	

α_{wt}	working pressure angle	[deg]
γ	C_p/C_v: adiabatic constant	
ε	compression ratio	
η_{em}	electric motor efficiency	
η_{di}	diesel engine efficiency	
η_{fc}	frequency converter efficiency	
η_{gen}	genset efficiency	
η_{gb}	gearbox efficiency	
η_h	hull efficiency	
η_j	jet efficiency	
η_o	Open water efficiency	
η_{tot}	drivetrain total efficiency	
η_r	relative rotative efficiency	
η_{rs}	drivetrain residual efficiency	
μ_{mz}	mean coefficient of gear friction	
ρ	fluid density	[kg/m^3]
φ	injection ratio	
ω	angular frequency	[rad/s]

1 INTRODUCTION

Major part of international logistics and business is carried out by shipping goods across the globe using a vast fleet of commercial ocean-going ships. According to the Finnish customs agency, in year 2019, 91.9 % of import and 78.4 % of export to and from Finland, were transported by sea [1]. Although ships produce a mere 2.5 % of global greenhouse emissions, are daily fuel consumptions of a single ship in the scale of several tons. As fuel prices are a major financial cost to a shipping company, by the time of writing this work, the fuel price of very low sulfur fuel oil was priced at 532$/1000 kg at the global 20 port-index rating [2]. Daily fuel costs can, therefore, easily reach up to tens of thousands of US dollars on larger ships, even a small increase in efficiency can therefore save the ship operator vast amounts of money and help cut the greenhouse emissions of a single ship substantially.

International maritime organization (IMO) and its *marine environmental protection committee* (MEPC) in their 76th meeting adopted new annexes to the *International Convention for the Prevention of Pollution from Ships* (MARPOL), the amendments introduce mandatory indexes for energy efficiency indexes both in newbuild ships and existing ships [3]. The *Energy Efficiency Existing Ship Index* (EEXI) and *carbon intensity indicator* (CII) are required for existing ships above 400 gross register tons, from 1.1.2023 onwards. A similar index *The Energy Efficiency Design Index* (EEDI), has been implemented on newbuild since 2013 [4]. The EEXI and EEDI indices tell in practice how much a ship emits carbon dioxide emissions per transport capacity ton of cargo per nautical mile. Both of these indices are calculated once, whereas the CII is calculated annually and reviewed if a ship meets its reference value. The underlying principle is that ships are built and operated more effectively, and the effectivity is transformed into a quantifiable value.

Practically every new-built merchant ship built today is equipped with a reciprocating diesel engine to provide the required propulsion power to the drivetrain. Some ships, however, use gas engines instead of diesels. The difference, however, is minimal and the engine body may be exactly the same. Steam machinery in the form of steam turbines is primarily found on larger naval vessels, such as aircraft carriers. Gas turbines can be found on smaller and medium sized naval vessels such as destroyers and littoral combat vessels.

1.1 Scope of this work

The scope of this work is to define components causing inefficiencies on a commercial ship and create a calculation model to estimate ship efficiency and fuel consumption. As a major part of a ship's efficiency is built in a ship at the design phase, the goal of this thesis is to find the most efficient technical lay-out for a ship in a specific use. Efficiency in this scope, simply means the most energy efficient system, practically, minimizing the fuel consumption of the vessel without drop in speed compared to a reference ship property. Technical solutions to be maximized in efficiency in this thesis are the electrical power generating plant, propulsion motor and the possible use of a shaft generator in order to increase efficiency. The secondary aim of this work is to increase the reader's understanding of ship operation, construction and components that together make a functioning ship.

1.2 Research problems

The research problems in this work are summarized into two main questions:

- *"What kind of technical solutions and manufacturers exist today within the maritime industry in the multi-megawatt class of electric drives?"*
- *"How much could the total efficiency be improved by using shaft generators or diesel-electric drivetrain compared to a conventional set of ship components?".*

The hypothesis of the author is that it is possible to increase the total efficiency in every case described further in chapter 3.2. However, the largest increase in efficiency is reachable with vessels with the highest variability in load.

1.3 Research methods used in this work

The research methods used in this work consists of a series of e-mail interviews to shipping companies, operators, shipyards and naval architect companies as well as a literature review of ship construction and shipbuilding. With the information gathered by the interviews and the literature review, a fleet of four reference ships are modelled. The four ships consist of a harbor tug, large oceangoing containership, small bulks-cargo ship and a passenger ship. The fleet of ship types is chosen to have a maximum amount of variance in both propulsion- and electrical load as well as operational cycle.

The aim of the interviews is to find out how a certain type of ship is operated and how these ships are technically arranged and why a certain technical arrangement is chosen. Based on operational and constructional information received, the four reference ships are modelled with a theoretical fixed route and a load profile to fit this route and typical electricity consumption. The aim of the literature review is to find off-the-shelf technical solutions within the maritime industry. The technical solutions discovered in the literature review, are then cross-referenced with the results of the email interviews, and the theoretical reference ships are being modelled with a conventional combination of off-the-shelf products.

When the theoretical reference ships have been modelled to the extent of their operational environment, operational load profile and technical arrangement, a second set of four theoretical reference ships of similar type are modelled to have identical operational environment and load profile but are modelled with a technical arrangement considered hypothetically to be more efficient. The ships fuel consumption is then calculated over a reasonable operational period and the results in fuel efficiency are then compared with the ships respective counterpart.

1.3.1 Interviews

Two types of inquiries are sent to different types of companies within the maritime industry. Shipping companies and ship operators' interviews consists of information inquiries including:

- *"What kind of route does your ship travel?"*
- *"What is your main engine type in terms of power, rotational speed, number of engines and how many shafts do you operate?"*
- *"Number and power of auxiliary engines?"*
- *"Does your ship have a shaft generator?"*
- *"What kind of load profile does your ship have in terms of propulsion and electrical load?"*
- *"Is it possible from operational point of view to have some number of main engines on stand-by on your normal route and operation if appliable to your ships construction?"*

Shipyards and naval architect companies' interviews consists of information inquiries such as:

- *"How is the total propulsion power estimation carried out in the design phase in shipbuilding?"*
- *"What kind of operational requirements dictate the arrangement of drivetrains in a ship?"*
- *"When is a shaft generator considered a feasible choice, and what are the design features involving such a decision?"*
- *"How does the possible existence of a shaft generator affect the amount of installed electrical power on auxiliary engines?"*

1.3.2 Literature review

The main goal of the literature review is to increase understanding about technical solutions and makers available within the maritime industry at time of writing this work. Technical solutions under research include marine engines and their manufacturers, complete generator sets or separate generators to match the marine engines previously discovered, shaft generators and their auxiliary equipment, electrical propulsion systems and thrusters. The literature review on these components and systems is mainly focused on finding quantifiable technical specifications to the systems, these specifications include maximum and maximum continuous power and total efficiency.

In order to find the maximum efficiency of a ship, some effort needs to be put into the research in the drivetrain efficiency, especially the powertrain and propeller efficiency. Since the hypothesis of the author is that the choice of the propulsion motor (electrical vs. reciprocating piston internal combustion engine) and operational requirement solely dictates the type and arrangement of the drivetrain, therefore efficiency calculations must include the complete system. The efficiencies of the diesel engines used in the maritime industry are discussed briefly, although technical solutions exist to power ships using gas- and steam turbines, this thesis is focused on using diesel engines as primary source of power.

One must understand that decarbonization of shipping will also take place but most probably all long-distance ships will use the thermodynamically most efficient diesel cycle also in the future. In such a case synthetic diesel has to be used. One, maybe easier, option, of course

is, that future ships will travel burning synthetic methane in gas engines. For example, Wärtsilä offers already engines that are converted to burn methane. Methane has a high compression durability and therefore the Otto principle can be used in an originally diesel engine that has the same compression ratio the same charge pressure and same efficiency as the diesel engine. The only difference is that the air-gas mixture is ignited either with a small diesel fuel injection or with a spark plug. Diesel-ignited motors are offering, at least in principle, a bi-fuel operating capability. If there is no methane in the compressed air diesel injection can be turned to deliver full power.

From the power-to-x -point of view methane is more interesting fuel than synthetic diesel as the efficiency of methane production is clearly higher than the efficiency of diesel production. Therefore, methane offers a higher solar electricity to ship propulsion efficiency than synthetic diesel.

There are also other future fuels that can be utilized in diesel engine -based future engines. Ammonia or methanol are alternatives of interest. In addition, there is lots of research and development work about using hydrogen in piston engines. All these fuel alternatives that suit the present-day motor with small modifications point in the direction that piston engines will be used in shipping also in the future.

2 SHIP EFFICIENCY FACTORS

In this chapter a basic knowledge of ship efficiency and operation is discussed, efficiency of each component of a ship's drivetrain is briefly explained and a basic knowledge in propulsion power estimation is explained.

2.1 Power requirement of a ship and design aspects

Moving a ship through water in general requires a lot of power, the sheer size and speed requirements of most ships dictate that the need for power in most cases exceeds several megawatts. The thrust of the ship needs to overcome the total resistance of the ship's hull, to achieve the design speed. The thrust of the ship is the rotative power of the propeller converted into forward driving force.

The ship's hull is the basis for all design in the ships propulsive power plant. By defining the ships service speed and function, consequently defining the geometry and the speed that this geometry needs to move through water, the designer of the ship defines at the same time the design parameters needed in the design process of the propeller and the propulsion plant. Since the propeller and the ship's hull are in close vicinity of each other, and the propeller usually is in the aft part of the ship, the hull design has a fundamental impact on the waterflow entering the effect area of the propeller. [5]

The geometry of the ship together with the speed of the ship also defines the resistance of the ship. The resistance of the ship can be estimated, and usually in the predesign phase of the ship using a database of model ship and real size ship sea- and basin trials, from which by adjusting design parameters to fit the newbuild, the resistance of the ship can be relatively accurately estimated. Some regression-based equations and calculation methods exist to estimate the drag of the hull, most famous and useful of these would be the Holtrop-Mennen method, described in detail in for example [5] chapter 50 and [6]. Later in the design phase, when the final hull structure is known, the hull is analyzed using *Reynolds-averaged Navier-Stokes based Computational fluid dynamics* -analysis (later in this paper referred as RANS CFD), from which the final resistance of the hull is obtained. [7] [8]

According to [9] the total resistance of the ship is divided into three groups:

1. Frictional resistances

2. Residual resistances (pressure resistance)
    a. Eddy resistance (transom immersion resistance)
    b. wave resistance
3. Air resistance

For low-speed ships, the most dominant of these is the frictional resistance. For slower ships, the percentage for the frictional resistance of the total the total resistance can be as high as 90 %, whereas for high-speed ships the frictional resistance can be as low as 45 %. The force acting against the thrust generated by the propeller of the ship, follows the general Bernoulli's principle of dynamic pressure, and increases drastically with the speed of the vessel. [9]

The Holtrop-Mennen resistance estimate method results in total resistance for the ship under specified conditions. The method composes the total resistance followingly:

$$R_{\mathrm{T}} = (1 + k)R_{\mathrm{F}} + R_{\mathrm{app}} + R_{\mathrm{A}} + R_{\mathrm{W}} + R_{\mathrm{B}} + R_{\mathrm{TH}} + R_{\mathrm{TR}} + R_{\mathrm{AA}} \quad (1)$$

when R_T: total resistance [N],
R_F: frictional resistance [N],
R_{APP}: appendage resistance [N],
R_W: wave resistance [N],
R_B: bulbous resistance [N],
R_{TR}: transom resistance [N],
R_{TH}: thruster tunnel resistance [N],
R_A: model-ship correlation resistance [N],
R_{AA}: air resistance [N],
k: hull form factor.

The frictional resistance is the resistance of liquid layers shearing between each other, in essence, the resistance caused by the viscosity of the fluid in which the vessel is travelling. The appendage resistance is the pressure resistance caused by extremities of the vessel (stabilizer fins, propeller shafts and their brackets, keels, rudders, etc.) interacting with the fluid. Wave resistance is the energy lost to the waves caused by the vessel in motion, the wave in question is composed of the wave in the aft of the ship and the "wave wall" at the fore of the ship. The bulbous resistance is an additional resistance caused by the possible bulb of the ship. Transom resistance is the resistance caused by the low pressure drag caused

by the transom of the ship if submerged. The transom of a vessel is the vertical part of the aft designed to strengthen the ships structure in the aft. The thruster tunnel resistance is the pressure resistance caused by the thruster tunnel. The model correlation resistance is composed of the residual resistance components and hull roughness resistance. Air resistance is the resistance caused by the ships structures that are exposed to air moving through air. For a 144 meter long vessel, table 1 shows the corresponding resistance components and their estimated value.

Table 1) Resistance components for a 144m meter long vessel travelling at 17.5 kn

R_{AA}	R_A	R_{APP}	R_B	R_F	R_W	R_{TH}	R_{TR}	R_T
80.2 kN	15.2 KN	4.57 kN	38.8 kN	27.6 kN	11.0 kN	0	0	58.3kN

By knowing the total resistance of the ship at a certain speed, the propeller power can be calculated. The connection between ship resistance and propeller thrust is [8]:

$$F_{\mathrm{pr}} = \frac{R_{\mathrm{tot}}}{(1-t)} \tag{2.0}$$

when F_{pr} propeller thrust [N],

t thrust deduction factor, typically 0.15…0.25,

The power necessary to propel the ship at the design speed is then defined as [8]:

$$P_{\mathrm{D}} = v_{\mathrm{s}} R_{\mathrm{tot}} \frac{1}{\eta_{\mathrm{o}} \eta_{\mathrm{r}} \eta_{\mathrm{h}}} \tag{2.1}$$

when P_{D} power absorbed by the propeller [W],

v_{s} speed of the vessel [m/s],

η_{o} propeller open-water efficiency, typically 0.35…0.7,

η_{r} relative rotative efficiency, typically 0.95 … 1.05,

η_{h} hull efficiency, typically 0.95 … 1.05.

Propeller open-water efficiency calculation is based on Wageningen-series data [10]. Relative rotative efficiency and thrust deduction factors are results of Holtrop-Mennen method [6]. The thrust deduction factor corresponds to the difference in a towed ship and a ship that is propelled by a propeller. A propeller increases velocities around the hull which would not be present if the ship is towed. The difference in these velocities create additional drag in the aft part of the ship, and therefore a thrust deduction factor is necessary. The

relative rotative efficiency is a factor describing the differences in torque absorption abilities when a propeller operates at similar conditions in a mixed wake and open water flow. Since propeller data is acquired from test conducted at ideal (uniform) wake, an efficiency factor is required to describe the change of efficiency when propeller works in conditions behind the hull. For single propeller vessels, the relative rotative efficiency can even exceed unity [5]. Hull efficiency is defined as: [8]

$$\eta_{\mathrm{h}} = \frac{(1-t)}{(1-w_{\mathrm{a}})} \tag{3}$$

when w_{a} hull wake fraction obtained from Holtrop-Mennen method, CFD-computation or Taylor's method, typically w_{a} is in the range of 0.1… 0.3.

2.2 Efficiencies of ship components and construction of a ship

In this chapter, the efficiencies of a ship's drivetrain are discussed. The drivetrain of the ship in this thesis is simplified to the prime mover, in this case a diesel engine of either a four-stroke trunk piston type engine or a two-stroke crosshead type engine. Further along the drivetrain is the gearbox, which in a diesel-driven ship reduces the rotational speed of the driveshaft to fit the rotational speed of the propeller. The mechanical power is transferred to the propeller by shaft lines, which need to be supported by radial and thrust bearings and possible bulkhead seals. These form the residuary losses, typically 2% of total input power. The final part of the drivetrain is the propeller, which converts the rotational power generated by the prime mover into thrust that moves the ship.

On a diesel-electric ship, the drivetrain of the ship is constructed of the diesel-engine coupled to an AC-generator forming a generating set. Further along the drivetrain is a frequency converter which drives the electric motor which mechanically drives the propeller.

The total efficiency of the mechanical drivetrain:

$$\eta_{\mathrm{drt}} = \eta_{\mathrm{di}}\eta_{\mathrm{gb}}\eta_{\mathrm{rs}} \tag{4}$$

when η_{drt} drivetrain total efficiency,

η_{di} diesel engine efficiency, typically 0.4 … 0.5,

η_{gb} gearbox efficiency, typically 0.97,

η_{rs} drivetrain residual efficiency, typically 0.98,

and respectively the efficiency, the diesel-electric drivetrain:

$$\eta_{\mathrm{drt}} = \eta_{\mathrm{gen}}\eta_{\mathrm{fc}}\eta_{\mathrm{em}} \tag{5}$$

when η_{gen} genset efficiency, typically 0.37 … 0.48,

η_{f} propulsion motor frequency converter efficiency, typically 0.97,

η_{em} electric propulsion motor efficiency, typically 0.98 in MW range.

Within the industry, a widely spread rule of thumb exists that a mere third of all the energy supplied to the engine in the form of fuel, is transformed into kinetic energy, or to the speed of the ship [3]. Therefore inversely, two thirds of the energy are lost in the form of mostly heat due to inefficiencies in the systems of the ship.

2.2.1 Efficiency of a diesel engine

In 1893 Rudolf Diesel patented the diesel engine in Germany, and the fundamental working principle of the engine has not changed in over a hundred years. The diesel process is based on high-pressure injected hydrocarbon fuel self-ignited by the temperature risen by the adiabatic compression of scavenged air in the cylinder by the working piston. The fuel oil is injected just prior to the top-dead-center (TDC) of the piston action, and the finely dispersed fuel is self-ignited by the heat, the pressure of the expanding gases generated by the burning hydrocarbons force the piston downwards, thus – with the help of crankshaft – creating rotational torque and therefore power. Ideally, the gases produced in the burning process are carbon dioxide and water vapor, and due to unwanted residues in the fuel and imperfect burning process, gases such as sulfur dioxide, carbon monoxide and microscopic particulates are generated. [9] Depending on the burning temperature, also nitrogen in the burning air may create oxides which is regarded as one of the biggest problems of the diesel engine these days and many modifications in the motor design and flue gas treatment have been taken in practice to reduce nitrogen oxides in the flue gases emitted in the atmosphere.

The ideal process is given graphically in figure 2:

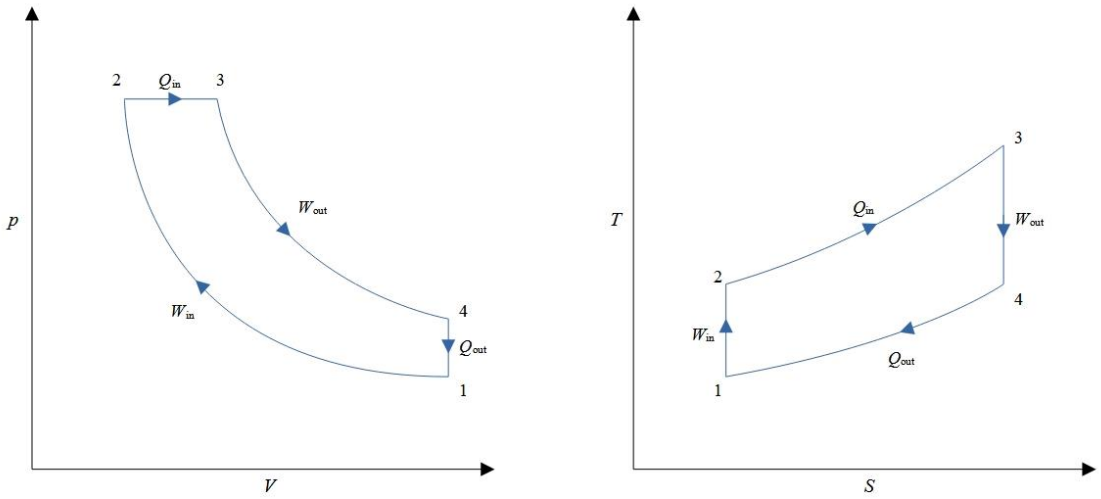

Figure 1) pV- and TS-graph (pressure p, volume *V*, temperature *T*, entropy *S*) of the ideal diesel process, reproduced from [11] and [9]. Q_{in} and Q_{out} are input and output energy per cycle and W_{in} and W_{out} are the mechanical works done by the piston.

The *pV*-graph indicates the compression and power cycles of the engine. The compression cycle starts from point 1 where the inlet air valve is closed, as work W_{in} is done by driving the piston closer to top dead center (TDC), the volume *V* decreases, and pressure *p* rises. At point 2, the fuel injection cycle starts, the fuel injection pump feeds the cylinder with fuel for given amount of piston movement. In ideal situations, the pressure is constant between points 2 and 3, as the piston is moving downwards increasing the volume between the piston top and cylinder head. At point 3, the fuel injection cycle ends, and the piston is forced downwards by the pressure inside the cylinder, doing work W_{out}. At point 4, the exhaust valve is opened, and the remaining pressure is, in principle, released into atmospheric pressure. In practice, there are no marine diesels without turbocharging. But the turbocharging itself does not affect the thermal efficiency of the diesel process, no changes are made to the compression ratio injection duration, this is clear from formula (1) and the *TS* drawing of the process. Of course, the turbocharger lowers the temperature of the exhaust gases and thus turns the energy into boost pressure, which allows more air and fuel to be injected into the cylinder for additional work, because there is more combustion air. Exchange of gases, i.e., the exhaust stroke and inlet stroke occur between points 0 and 1.

The *TS*-graph indicates the change of temperatures *T* and entropy *S* inside the cylinder during a full work cycle. The compression between points 1 and 2 is adiabatic, which means that no exchange of heat energy occurs between the system in question and its surrounding. Since no external heat is imported at this point, the change of entropy is zero. The temperature and pressure, however, are increased by [11]:

$$\frac{p_1}{p_2} = (\frac{V_2}{V_1})^{\gamma} \rightarrow \ p_2 = p_1(\frac{V_1}{V_2})^{\gamma} \tag{6}$$

$$\frac{T_1}{T_2} = (\frac{V_2}{V_1})^{\gamma-1} \rightarrow \ T_2 = T_1(\frac{V_1}{V_2})^{\gamma-1} \tag{7}$$

when γ: $C_p/\underline{C}_v$: 1.40: heat capacity ratio for air (adiabatic constant).

At point two, the injection cycle begins, the pressure is kept constant until point 3. As the volume is increased and pressure kept constant, the only thing that can allow this is the increasing heat of the gas inside the cylinder. The change in temperature according to ideal-gas theory is [11]:

$$T_3 = \frac{V_3 T_2}{V_2} \tag{8}$$

Since the change is no longer adiabatic, but isobaric, the change of entropy is no longer zero [11]:

$$\mathrm{d}S \ = \ m_a C_p \ln\left(\frac{T_3}{T_2}\right) \tag{9}$$

when m_a: the mass of the air inside the cylinder, [kg]

C_p: specific heat capacity under constant pressure.

Between points 3 and 4, the entropy is constant, and the pressure and temperature decreases as the volume increases adiabatically [11]:

$$\frac{p_3}{p_4} = (\frac{V_4}{V_3})^{\gamma} \rightarrow \ p_4 = p_3(\frac{V_3}{V_4})^{\gamma}$$

$$\frac{T_3}{T_4} = (\frac{V_4}{V_3})^{\gamma-1} \rightarrow \ T_4 = T_3(\frac{V_3}{V_4})^{\gamma-1}$$

Between points 4 and 1, the pressure inside the cylinder is released into atmospheric pressure under constant volume and the temperature settles at the atmospheric temperature, whilst the entropy is reduced to the entropy at point 1 as [11]:

$$\mathrm{d}S = m_\mathrm{a} C_\mathrm{v} \ln\left(\frac{T_1}{T_4}\right)$$

when C_v specific heat capacity under constant volume.

The efficiency η_di of the ideal diesel process is famously given as [11]:

$$\eta_\mathrm{di} = 1 - \frac{1}{\varepsilon^{\gamma-1}} \frac{\varphi^\gamma - 1}{\gamma(\varphi - 1)} \tag{10}$$

when η_di diesel engine efficiency,
φ V_3/V_2: injection ratio,
ε V_1/V_2: compression ratio.

Despite the working principle and therefore the theoretical efficiency eq. (10) [11] of a diesel engine is quite simple, the formula for ideal efficiency neglects the losses of the engine caused by for example friction losses in the bearings, piston and the cylinder or losses caused by the fuel injection mechanism, coolant- and lubricating pumps. Also eq. (10) does not take into account the existence and work done by the turbocharger of the engine. The turbocharger converts the energy released into the atmosphere in figure 1 energy exiting out of the system at Q_out into charge air going into the engine again. The turbocharger, therefore, does not increase the efficiency of the diesel process, but it forces more air in a cylinder and therefore enables injection of more fuel (increase of injection ratio) which results in a significantly higher power than with a naturally aspirated engine. According to eq. (10) an increase in injection ratio should decrease the efficiency of the diesel process since it increases the unused energy Q_out exiting the system.

However, the turbocharger uses at its own work process this same energy Q_out, decreasing the negative impact of the injection ratio increase on the diesel process efficiency and thus increasing the total efficiency of the plant by harvesting lost energy by the diesel process in the turbocharging process. A decrease in fuel injection ratio increases the diesel process efficiency, but at the same time decreases the energy harvestable by the turbocharger. And

vice versa. A naturally aspirated engine and a turbocharged engine share exactly the same *TS*-graph, given that the input air temperature, injection- and compression ratios remain the same (therefore a turbocharged engine needs an intercooler). [9]

The induced power of the engine is calculated using mean induced pressure, from the actual measured *pV*-graph of the engine. The *pV*-graph is gained using a pressure sensor connected to a specific indicator valve on the engine, to open a port into the cylinder chamber. The sensor usually calculates the mean induced pressure directly and draws a *pV*-graph of the engine. The power of the engine is calculated using a formula known within the industry as the engine formula [9]:

$$P_{\mathrm{i}} = \frac{\pi}{4} D_{\mathrm{pi}}{}^{2} s_{\mathrm{pi}} \frac{n}{a} Z_{\mathrm{c}} p_{\mathrm{i}} \tag{11}$$

when P_{i} induced power [W],

D_{pi} piston bore [m],

s_{pi} piston stroke [m],

n crankshaft rotational speed [1/s],

a: constant depending on engine type, a = 1 for two-stroke and a = 2 for four-stroke,

$\mathrm{Z_c}$ number of engine cylinders,

p_{i} mean induced pressure [Pa].

The indicated power output is calculated using pressure values recorded from the combustion chamber, and therefore consequently, indicate only the amount of power to be harvested from the fuel in the form of mechanical work. The induced power still contains the mechanical losses of the engine. The mean induced pressure and power are useful factors in determining the condition of the engine, sudden drop in induced power may indicate faults in fuel injection system or the valves. The only way of fully determining the efficiency of the engine is by comparing the mechanical power output to the total energy supplied in the form of fuel. This can be calculated by:

$$\eta_{\mathrm{di}} = \frac{P_{\mathrm{m}}}{F_{\mathrm{c}} C_{\mathrm{f}}} \tag{12}$$

when P_{m} mechanical power [W],

f_{c} Fuel consumption [kg/s],

C_f Fuel specific energy [J/kg],

Engine manufacturers generally indicate the engines total efficiency in the form of *specific fuel consumption,* or SFC. SFC is standardized by ISO 3046-1:2002. The most common unit of SFC indicated is grams/kWh. As an example, when using the fuel specific energy of 42.78 MJ/kg and the SFC provided by Wärtsilä [12], the total efficiency of a Wärtsilä 8V31 engine is:

$$\eta_{di} = \frac{1\ \text{kWh}}{SFC \cdot C_f} = \frac{3600000\ \text{Ws}}{0.1677\ \frac{\text{kg}}{\text{kWh}} \cdot 42780000\ \text{J/kg}} = 0.5018$$

The efficiency of the diesel engine is correlated to the size of the engine, the larger the engine the better the efficiency. This is due to relation of the radiant surface area and the volume of a cylinder. An increase in cylinder bore produces a relatively smaller increase in cylinder surface area than cylinder volume and, therefore a relatively smaller amount of heat can escape to the cylinder surroundings, and consequently a larger amount of heat is transformable into work [9]. The most efficient internal combustion engines are 2-stroke diesel engines, capable of producing 80 MW of power. Such engines can reach efficiency slightly higher than 50%. Table 2 lists properties of some marine engines.

Table 2) A list of technical specifications for some of the most successful marine diesel engines.

	Wärtsilä X92-B (Produced under license to WinGD) [13]	MTU 12V 4000 M73L [14]	MTU 16V 8000 M91L [15]	CAT 3512E [16]	Wärtsilä 31-series [12]	Wärtsilä 46-series [12]	MaK M43C-series [17]	MAN B&W G95ME-C10.6-HPSCR [18]
Specific fuel consumption [g/kWh]	163.8	213	198	196.3	167.7	175	177	161
Cylinder bore [mm]	920	170	265	170	310	460	430	950
Cylinder stroke [mm]	3468	190	315	215	430	580	610	3460
rotational speed [1/min]	80	2050	1150	1800	750	600	500	80
Mean eff. pressure [bar]	21	NA	NA	NA	30.1	24.9	27.1	21.0
Cylinder output [kW/cyl.]	6450[1]	180[1]	500[1]	158.4[1]	610	1200	1000	6870[1]
Efficiency (calculated using eq. (3))	0.514	0.395	0.425	0.429	0.502	0.481	0.475	0.523

1) Calculated from total output power.

Figure 2 illustrates the specific fuel consumption and cylinder diameter of Table 2 engines. The engines are sorted by the cylinder bore, with the highest cylinder diameter on the left on figure 2.

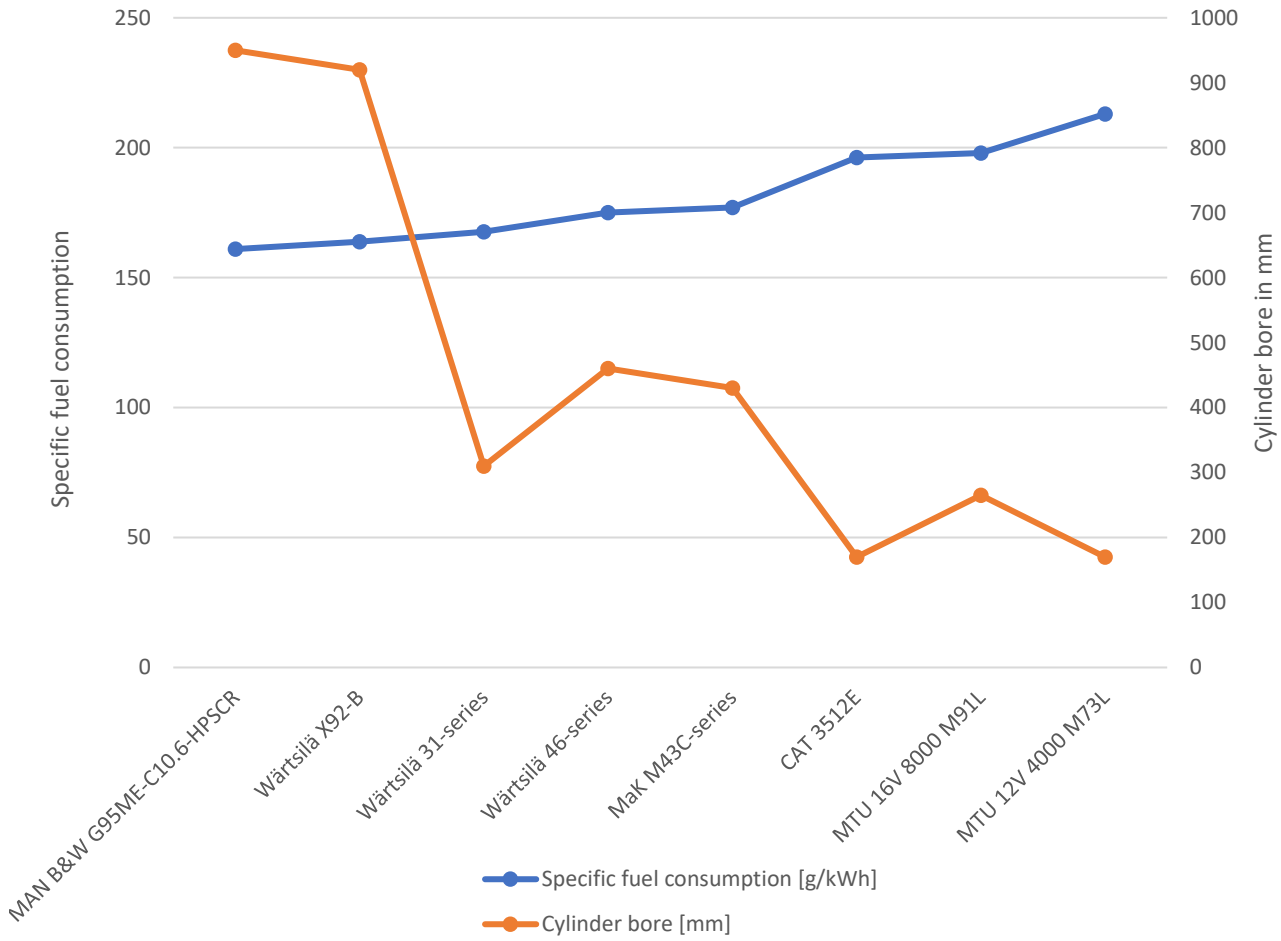

Figure 2) Fuel consumption and cylinder bore size.

However, the specific fuel consumption is not constant for the entire power range. The engine manufacturer usually states only the *best specific fuel consumption*-value (or BSFC-value in some literature). The lowest value for SFC is located usually in 75 – 85 % region of the engine peak power.

[19] introduces guidelines to mapping SFC-values for an engine. Table 3 gives specific fuel consumption values at engine different speeds and torques used in this thesis for computations in later phase. The table is produced to represent a typical engine behavior for PU-values of the best SFC value.

Table 3) Engine per-unit specific fuel consumption. Table is produced by the author to represent the example calculations in PU-values in [19]. The optimum point is found at 0.7 per unit speed and 0.8 per unit torque.

PU rot. speed \ PU engine torque	0.1	0.2	0.3	0.4	0.5	0.6	0.7	0.8	0.9	1	1.1
0.1	4.418	3.195	2.676	2.390	2.208	2.261	2.183	2.338	2.079	2.079	2.079
0.2	3.587	2.363	1.973	1.804	1.667	1.678	1.657	1.667	1.688	1.688	1.688
0.3	3.177	2.112	1.794	1.588	1.458	1.364	1.321	1.280	1.308	1.495	1.495
0.4	2.828	1.886	1.594	1.431	1.311	1.234	1.166	1.166	1.183	1.251	1.371
0.5	2.485	1.699	1.427	1.267	1.186	1.098	1.090	1.090	1.090	1.138	1.283
0.6	2.201	1.541	1.313	1.176	1.108	1.078	1.047	1.032	1.032	1.093	1.214
0.7	1.884	1.369	1.159	1.130	1.116	1.077	1.043	1.000	1.028	1.058	1.159
0.8	2.019	1.378	1.228	1.177	1.093	1.065	1.016	1.008	1.016	1.030	1.114
0.9	2.016	1.465	1.312	1.183	1.095	1.042	1.015	1.008	1.019	1.028	1.075
1	2.474	1.667	1.367	1.205	1.107	1.029	1.025	1.009	1.024	1.029	1.042
1.1	2.657	1.797	1.481	1.284	1.152	1.038	1.050	1.038	1.025	1.019	1.012

2.2.2 Efficiency of a gearbox

Despite the low speed of large diesel engines, the speed is far too high for a high-efficiency propeller. Therefore, a gear is often needed. Only the biggest two-stroke engines may drive a high-diameter propeller directly.

The efficiency of a marine gearbox is generally quite high. Molland A. et al. [20] state that in general the efficiency of the drivetrain in direct driven ships is 0.98 and gearbox driven systems 0.95. Given that the driveshaft in this instance consists of the shaft itself, its support bearings, shaft seal through the transom of the ship and possible bulkhead seals which would either way be a part of the structure whether the ship be equipped with a gearbox or not, states this that the efficiency of the gearbox itself in general cases would be in the range of 0.97.

A marine gear at its simplest consists of the primary and secondary cogwheels, clutch and its hydraulic pump, bearings, and usually at least one PTO possibility to drive for example a hydraulic pump to power ship rudder. In more complex configurations, the gear can have

multiple intakes of power, multiple outtakes of power, several pumps driving for example the rudder and clutches.

[22] researched the efficiency of automotive gearboxes with varying loads and speeds. The general conclusions of the experimental study showed that the gearbox efficiency is related to the input torque and speed. The highest efficiencies were achieved at higher values of input torque and lower rotational speed. The peak efficiency was 0.98. Correspondingly the lowest overall efficiency is achieved with a low input torque and highest rotational speed. The minimum overall efficiency value was 0.86. Obviously, one has to note that the experiment and its results were carried out with a gearbox designed to be used in the automotive industry, and the power handling capability, input torque and rotational speed are therefore mismatched for maritime use in this spec and has to be treated just as a indicative.

According to [23], the losses of a universal gearbox consist of no-load losses and load dependent losses. The no-load losses are losses related to the friction in seals, power demand of the auxiliaries, gearbox lubricant, its viscosity, and the lubricant contact to rotating the components, in essence the immersion depth of gears and bearings in a wet sump lubricated gearbox. The load-depending losses consist of frictional losses in the bearings and gears sliding against each other by the tangential force of the torque rotating the gearbox shafts. The power loss in a single gear is defined by [23] as:

$$P_{\mathrm{VZP}} = F_{\mathrm{t.max}} v_p \, \mu_{\mathrm{mz}} \frac{1}{\cos\left(\alpha_{\mathrm{wt}}\right)} \frac{1}{p_{\mathrm{et}}} \int_A^E \left(\frac{F_{\mathrm{N}}}{F_{\mathrm{N.max}}} \frac{v_{\mathrm{g}}(x)}{v_p} \right) \mathrm{d}x \tag{13}$$

when

P_{VZP}	load gear losses [W],
F_{t}	Tangential force [N],
v_{p}	pitch line velocity [m/s],
v_{g}	sliding velocity [m/s],
α_{wt}	working pressure angle [deg],
μ_{mz}	mean coefficient of gear friction,
p_{et}	transverse pitch [mm],
F_{N}	normal force [N].

With the integration limits *E* and *A* correspond to the path of contact between two gear teeth.

Pitch line in the SFS-ISO 1122-1-standard ”*Vocabulary of gear terms. Part 1: Definitions related to geometry*” is referred as *pitch circle*. The standard defines in practical terms this as the circle on the gear profile with the mean point of contact between two gear tooths. The pitch circle is illustrated in figure 3.

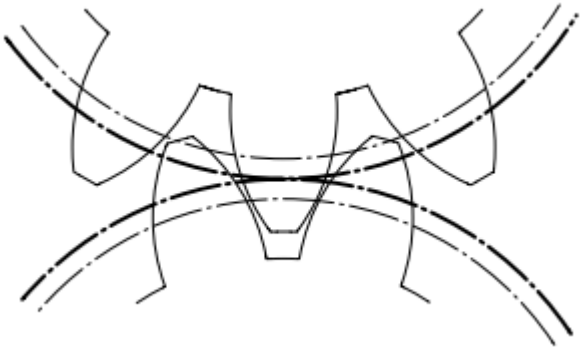

Figure 3) Pitch circle of a gear [24].

The sliding velocity in [25] is defined as *“At a point of contact of two tooth flanks in engagement, the sliding speed, v_g, is the difference of the speeds of the two transverse profiles in the direction of the common tangent.”* Figure 4 shows the composition and the sliding velocity in the interaction between two cogwheels.

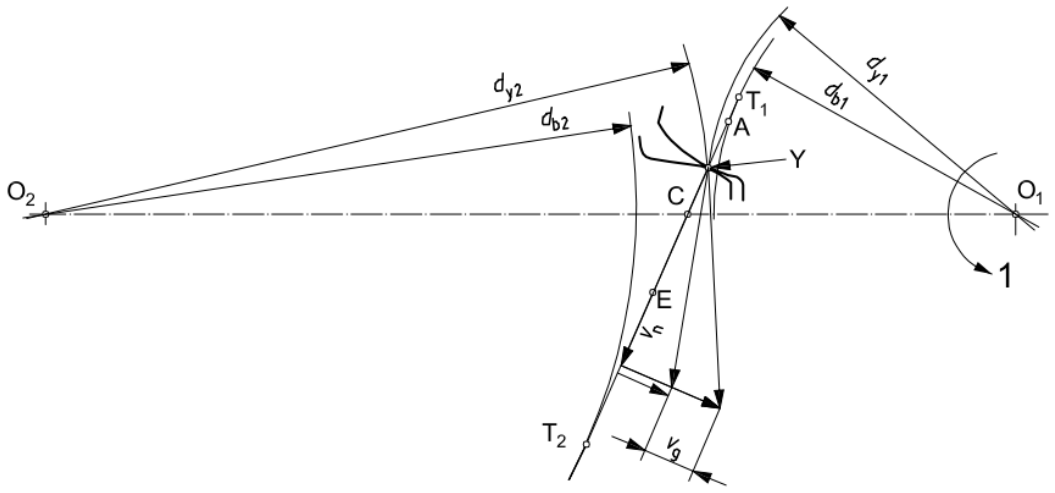

Figure 4) Vector presentation of gear sliding velocity [25].

Transverse pitch is defined as the length between two corresponding points between two adjacent teeth. Figure 5 shows the definition of transverse pitch graphically. [24]

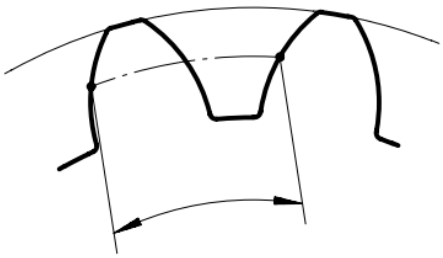

Figure 5) Transverse pitch of a cogwheel [24].

[23] states that for the part-load operation of the gearbox, the no-load losses are a dominant feature, whereas full load operation the major contribution for total losses are the gear mesh losses defined by eq. (13).

2.2.3 Efficiency of a propeller

John Ericsson invented the ship propeller in 1839 and patented it as US patent No: 588 (https://www.invent.org/inductees/john-ericsson). Later different versions of propeller have been introduced. Propeller efficiency study in this work consists of efficiency comparison of fixed pitch propellers (FPP), controllable pitch propellers (CPP) and rudder propeller systems. The concept of propeller blade efficiency will be discussed in short.

A propeller is a device that in a ship or a boat, transforms the rotational torque into thrust that propels the ship forwards. As the name dictates, the FPP has propeller blades that are in a fixed position on the propeller shaft, whereas the CPP has the ability to alter the blade angle in order to alter the amount of thrust generated by the propeller, while the propeller still rotates in the original direction. Rudder propeller systems are systems where the propeller is located on a vertical hub, which can be rotated around its axis to direct the thrust in any direction.

CP-propellers are complex in design compared to FP-propellers. The propeller hub on a CPP contains a hydraulic mechanism to alter the pitch on the propeller blades. This makes the propeller hub on the CPP larger compared to FP-propeller, this combined with the fact that the blades of the CPP need to be reversed in direction compared to forward motion and therefore cannot be overlapping in the design process, lowers, and limits the design

parameter A_e/A_o. This design parameter is known as the expanded area ratio, it is defined as total blade area A_e divided with the total propeller swept area A_o. In addition, the blade root area of the CPP is limited due to the reversibility demand, this faces a challenge of the mechanical stress of the blades. In order to endure the stress in the blade root, the root needs to be somewhat thicker than in an FPP. The larger hub reduces the effective propeller actuator disc area, which in turn reduces the jet efficiency of the propeller. Also, the demand for a rotational movement on the blade, requires a blade palm, which has a minor impact of generating turbulence. These factors combined makes the CPP somewhat lower in efficiency compared to FP-propellers [26] [9]. Figure 6 shows a typical CPP, its shaft and hub:

Figure 6) Controllable pitch propeller [22].

CP-propellers are especially beneficial in ships equipped with a shaft generator. A direct on-line electric machine in general requires the rotational speed to be fixed to a constant speed, in order to maintain constant frequency of the electrical network. If a shaft generator were to be installed on a ship equipped with a FPP, the ship would be constrained to only one engine rotational and therefore one ship speed, since the frequency of the electrical network is required to be constant. Alternatively, the shaft generator frequency can be altered using a frequency converter, however in this case the efficiency (about 97 %) of the frequency converter needs to be taken into account. By using a CPP, the rotational speed of the diesel engine, shaft, and consequently the frequency of the shaft generator without the use of frequency converter, can be kept constant and the thrust of the propeller can be altered freely by altering the pitch of the propeller blades. [27] [26].

The fundamental working principle can be expressed with the momentum theory, originally published and studied by [28]. In the momentum theory, the propeller is simplified to a homogenous actuator disc, and the fluid flow is considered incompressible, laminar and ideal. The fluid flow is constrained inside a slipstream, in essence, the actuator disc is considered to exist in a pipe with no leaks. The actuator disc produces thrust by creating a higher pressure on the outflow side of the actuator disc than the inflow side of the disc. This pressure acts on the actuator disc as a force moving the ship forward. Figure 7 shows graphically the flow of fluid across the actuator disc [28].

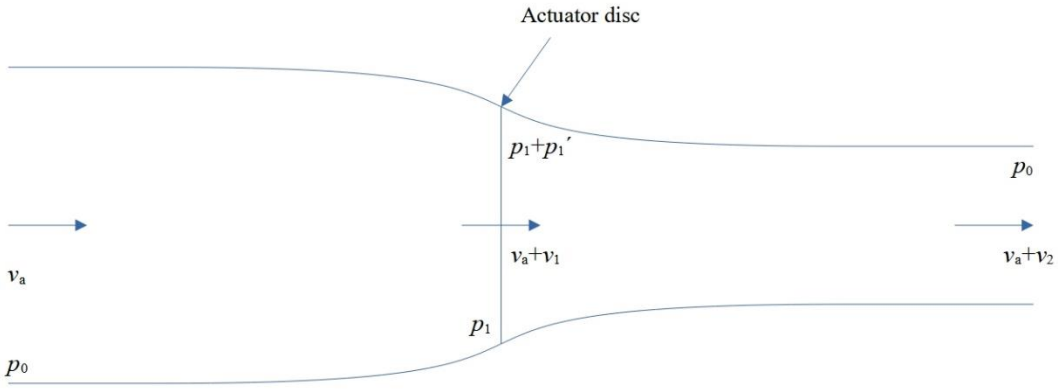

Figure 7) Momentum theory illustration and ideal propeller flow.

The fluid is moving from the inlet to the outlet, i.e. from v_a to v_a+v_2. The propeller is situated at the actuator disc, and the propeller area is written A_0. The thrust of the propeller is the defined [28]:

$$F_{pr} = A_0 p_2' \tag{14}$$

when F_{pr} propeller thrust [N],

A_0 actuator disc area [m^2],

p_2' pressure increase behind the actuator disc [Pa].

Since the principle of conservation off mass requires the volume V to be the same on either side of propeller at point 2, and the propeller increases fluid flow from inlet to outlet. Therefore, the volume of mass is longer but contracted on the outlet side of the propeller. The velocity of fluid just prior to the propeller is composed of v_a, and acceleration factor v_2. consequently, the velocity at the end of the slipstream is composed of a similar acceleration factor v_3 and the speed of advance [28].

As the flow of fluid approaches the propeller and accelerates to v_a+v_2 from the speed of advance v_a. At the same time, the pressure on the inlet side of the propeller reduces to p_2 from the surrounding static water pressure, $p_{1,}$ in which the propeller is situated. The velocity of fluid in the immediate vicinity of the propeller on the inlet and outlet side is constant, however the pressure in the immediate vicinity of outlet side of the propeller rises. This increment of pressure is equal to the thrust of the propeller. The pressure increase is slowly deteriorating with the slipstream and eventually equalizes with the surrounding pressure [28].

For the whole system with the previously defined simplifications, the Bernoulli's principle is applicable [28]:

$$H_0 = p_0 + \frac{1}{2}\rho {v_a}^2 = p_1 + \frac{1}{2}\rho(v_a + v_1)^2 \tag{15}$$

when p_0 ambient static pressure [Pa],

p_1 pressure prior the actuator disc [Pa],

v_a fluid velocity entering the system, speed of advance [m/s],

v_1 fluid velocity increase prior to the actuator disc [m/s],

H_0 dynamic head before the actuator disc [Pa],

ρ fluid density [kg/m^3].

And the same total head for the system prior to the actuator disc [28]:

$$H_1 = p_0 + \frac{1}{2}\rho(v_a + v_2)^2 = p_1 + {p_1}' + \frac{1}{2}\rho(v_a + v_1)^2 \tag{16}$$

when v_2 fluid velocity increase behind the actuator disc [m/s],

p_1 fluid pressure prior to the actuator disc [Pa],

$p_1´$ fluid pressure immediately after the actuator disc [Pa],

H_0 dynamic head of the system after the actuator disc [Pa],

and consequently [28]:

$${p_1}' = H_1 - H_0 = \rho\left(v_a + \frac{1}{2}v_2\right)v_2 \tag{17}$$

According to the principle of momentum conservation states that all changes in momentum are caused by external forces, since our system is considered ideal, all changes in momentum are caused by the thrust of the propeller into the flow of fluid. Therefore [28]:

$$F_{\mathrm{pr}} = A_0 \rho (v_a + v_1) v_2 \tag{18}$$

Since thrust in essence is force, and force is the factor of pressure and area, therefore pressure increment can be written [28]:

$$p_1{}' = \rho (v_{\mathrm{a}} + v_1) v_2 \tag{19}$$

by combining equations (17) and (19), we find that [28]:

$$p_1{}' = \rho \left(v_{\mathrm{a}} + \frac{1}{2} v_2 \right) v_2 = \rho (v_{\mathrm{a}} + v_1) v_2 \rightarrow v_1 = \frac{1}{2} v_2 \tag{20}$$

Hereby we can conclude that half of the velocity increase is generated before the propeller and half of it after the propeller. By combining equations (18) and (20), thrust is [28]:

$$F_{\mathrm{pr}} = 2 A_0 \rho (v_{\mathrm{a}} + v_1) v_1 \tag{21}$$

The increase of kinetic energy *E* in a time unit within the fluid accelerated aft wards is [28]:

$$E = \frac{1}{2} A_0 \, \rho (v_{\mathrm{a}} + v_1)((v_{\mathrm{a}} + v_2)^2 - {v_{\mathrm{a}}}^2) \tag{22}$$

$$E = \frac{1}{2} A_0 \, \rho (v_{\mathrm{a}} + v_1) \, (2 v_{\mathrm{a}} + v_1) v_1$$

And since:

$$v_2 = 2 v_1$$

then:

$$E = 2 A_0 \, \rho (v_{\mathrm{a}} + v_1)^2 v_1$$

by inserting equation (21):

$$E = F_{\mathrm{pr}} (v_{\mathrm{a}} + v_1)$$

This represents the work done into the fluid by the propeller. Since the propeller is a rotating machine onto which torque is delivered, the work done on a single time unit is also [28]:

$$\Omega T_{\mathrm{pr}} = F_{\mathrm{pr}} (v_{\mathrm{a}} + v_1) \tag{23}$$

when T_{pr} propeller torque [Nm],

Ω angular frequency of the actuator disc [rad/s],

the ideal efficiency of the propeller is defined as the total useful energy divided by the total energy used by the propeller as follows [28]:

$$\eta_j = \frac{F\, v_a}{\Omega T} = \frac{v_a}{v_a + v_1} \tag{24}$$

when η_j jet efficiency of the actuator disc.

By bearing in mind that v_2 represents the increase of fluid velocity flowing through the actuator disc, equation (24) shows that the ideal efficiency decreases as the fluid flow is increased. Therefore, a larger actuator disc area is preferable if additional thrust is required. The simplified model pictures the actuator disc without a driveshaft that rotates the actuator disc, in actual applications there is always a driveshaft and a hub on which the propeller blades are situated on. Therefore, a larger hub size has the tendency to lower the theoretical actuator disc area when diameter is kept constant, thus increasing the fluid flow rate if same thrust is maintained and consequently, lowering the efficiency.

For example, if we consider a pair of hypothetical propellers with the same thrust and only difference is that the other propeller has a 10% decrease in blade area. If one considers a propeller which operates in a speed of advance of a per unit (pu) value of $v_a = 1$, actuator disc area $A_0 = 1$ in pu and we give the example propeller a reasonable jet efficiency value of 0.7. Therefore, with eq (24) we have the increase of fluid velocity v_1:

$$\eta_j = \frac{v_a}{v_a + v_1} \rightarrow\ v_1 = \frac{v_a}{n_j} - v_a = 0.428$$

By using eq x and the principle of equal thrust in both cases gives us that:

$$F_{pr_1} = F_{pr_2} = 2A_0\rho(v_a + v_1)v_1 = 2A_{0_1}\rho\left(v_a + v_{1_1}\right)v_{1_1}$$

To solve the jet efficiency, the increase in fluid flow must be solved:

$$\frac{A_0}{A_{0_1}}(v_a + v_1)v_1 = (v_a + v_{1_1})v_{1_1} \rightarrow {v_{1_1}}^2 + v_a v_{1_1} - (\frac{A_0}{A_{0_1}}(v_a + v_1)v_1) = 0$$

with the quadratic formula, the positive root of the equation is 0.4645. The corresponding jet efficiency is therefore:

$$\eta_j = \frac{1}{1 + 0.4645} = 0.682$$

The jet efficiency is the efficiency that neglects all other impacts on total efficiency. Since the jet efficiency neglects the inefficiencies caused by turbulence, friction, cavitation, etc., it is therefore unachievable in practical applications and insignificant in a real propeller design process. It, however, shows the mechanism behind the theory of how a larger hub lowers the total efficiency. A CPP requires a hub size in the range of 0.3 – 0.32 of the propeller diameter. [29]

Figure 8 shows the difference in efficiency between a CPP and a FPP system. The computation is based on the Wageningen B-series [10], in the computation the CPP has the ability to alter its blade area to achieve the best possible efficiency of all the *P/D*-ratios applicable to the Wageningen B-series. A reduction of 3 % in overall efficiency has been made on the CPP across the entire advance ratio range, of these 2 % represents the reduction of jet efficiency and an additional 1 % reduction has been made to compensate for the thicker blades and irregular shapes in the blade root required for CPP mechanical structure. The FPP has the *P/D*-ratio of 1.4. [20] states that the CPP has a 2-3 % drop in efficiency compared to its FPP counterpart with similar properties, so calculations above may be in some case considered accurate.

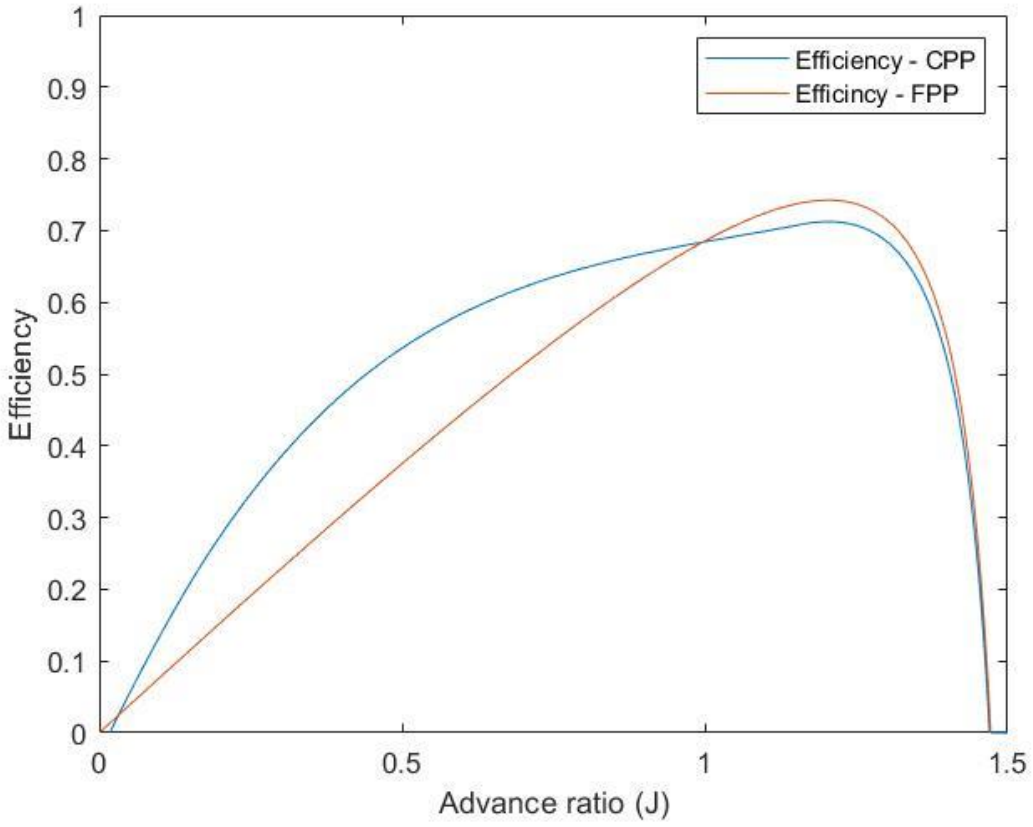

Figure 8) Efficiencies of a CPP and a FPP, computed with appendixes 2 and 3 ($J = \frac{v_a}{nD_{pr}}$)

In practical applications and real propellers, the propeller efficiency varies usually in the range 0.35 – 0.75. The higher values are reached with the design parameter advance ratio (J) at the higher values of its range. The advance ratio is a unitless design parameter defined as:

$$J = \frac{v_\mathrm{a}}{nD_\mathrm{pr}} \tag{25}$$

when n: rotational speed of the propeller [1/s],

D_pr propeller diameter [m],

v_a speed of advance [m/s].

The Speed of advance is the average fluid velocity experienced by the propeller. Since according to the concept of boundary layers in fluid dynamics, the fluid velocity in the close vicinity of the object moving in fluid is zero, the speed of water entering the propeller is always lower than the speed of the vessel. The Speed of advance can be calculated using modern computational fluid dynamics (CFD) in the same process as the drag calculations of the hull of the ship or with the Holtrop-Mennen method [6] as a part of the propeller-hull

interaction calculations. There are also some empirical formulas for estimating the wake fraction (w_a) other than Holtrop-Mennen method, which in Taylor's method is used to calculate v_a. The Taylor's method is probably easiest and simplest early design estimate of the wake fraction for propeller calculations [5]:

$$w_a = 0.5C_b - 0.05 \tag{26}$$

when C_b Block coefficient of the vessel,

and v_a is calculated using the ship velocity v_s and the Taylor's method [5]:

$$w_a = 1 - \frac{v_a}{v_s} \rightarrow v_a = (1 - w_a)v_s \tag{27}$$

The use of these empirical methods must be done with great caution, especially Taylor's formula for obtaining w_a, since they are not based on the hydrodynamical model of the flowing water around the vessel, the uncertainty and probability of error are considerable. They should be only used as a guideline or earliest possible estimate in the design process. [8]

The design process of the propeller is based on a wide series of open-water trials of model propellers, thus achieved a significant database of charts to select and manufacture a propeller to suit a specific project. The most widely used series for propeller design is known as the Wageningen B -series. The Wageningen B series consists of 120 propeller models, from which a regression analysis has created a series of polynomials to describe the properties of a propeller. [7] [10]

The fundamental of propeller design and calculation, is to determine the coefficients for thrust and propeller torque. Since the ship's hull has resistance that needs to be counteracted with the propeller thrust to move the ship forward, the thrust coefficient is an important design parameter. The propeller torque together with the rotational speed of the shaft determines the power delivered to the propeller, and with the thrust of the propeller already defined, the efficiency of the propeller can be written [10]:

$$\eta_o = \frac{J}{2\pi}\frac{K_F}{K_Q} \tag{28}$$

when η_o open water efficiency,
J advance ratio,
K_F thrust coefficient, typical values can be found in figure 10,
K torque coefficient, typical values can be found in figure 11.

The coefficients for torque and thrust have a following connection to the real propeller thrust and torque [10]:

$$K_F = \frac{F_{pr}}{\rho n^2 {D_{pr}}^4} \tag{29}$$

$$K_T = \frac{T_{pr}}{\rho n^2 {D_{pr}}^5} \tag{30}$$

when F_{pr} propeller thrust in [N],
T_{pr} propeller torque [Nm],
ρ water density [kg/m^3],
n propeller rotational speed [1/s].

From the original propeller model tests and the regression analysis, the thrust and torque coefficients are [10]:

$$K_F = \sum_{s,t,u,v} (C_{s,t,u,v.F} (J)^s (P/D)^t \left(\frac{A_e}{A_o}\right)^u (Z_{bl})^v \tag{31}$$

and:

$$K_T = \sum_{s,t,u,v} (C_{s,t,u,v.T} (J)^s (P/D)^t \left(\frac{A_e}{A_o}\right)^u (Z_{bl})^v \tag{32}$$

when P/D pitch/diameter ratio of the propeller,
A_e/A_o expanded area ratio of the propeller blades,
Z_{bl} number of blades on the propeller.

Equations (28) – (32) form the basis of the Matlab-codes in appendixes 2,3 and 4. The coefficients *s*, *t*, *u* and *v* can be found in the polynomials listed in appendix 1. The pitch/diameter ratio (*P/D*) is defined as the distance that the propeller would travel forward

during one rotation if there were no slip of the blades in water, divided with the propeller diameter. [9]

Figure 5 shows the effect of the propeller *P/D*-ratio on the propeller efficiency, a FPP would be constrained to only one of *P/D*-ratio, whereas CPP can freely alter its *P/D*-ratio by adjusting the pitch of the propeller. Figures 10 and 11 shows the corresponding torque and thrust coefficients for the same propeller. It is noticeable that the open water efficiency pictured in figure 9 is based on small scale model tests and their numerical analysis, and therefore the open water efficiency cannot be taken for a true propeller efficiency on a ship. The efficiency of a propeller is always dependent on the environment it is operating in, and therefore the efficiency of a propeller requires an analysis of the vessel.

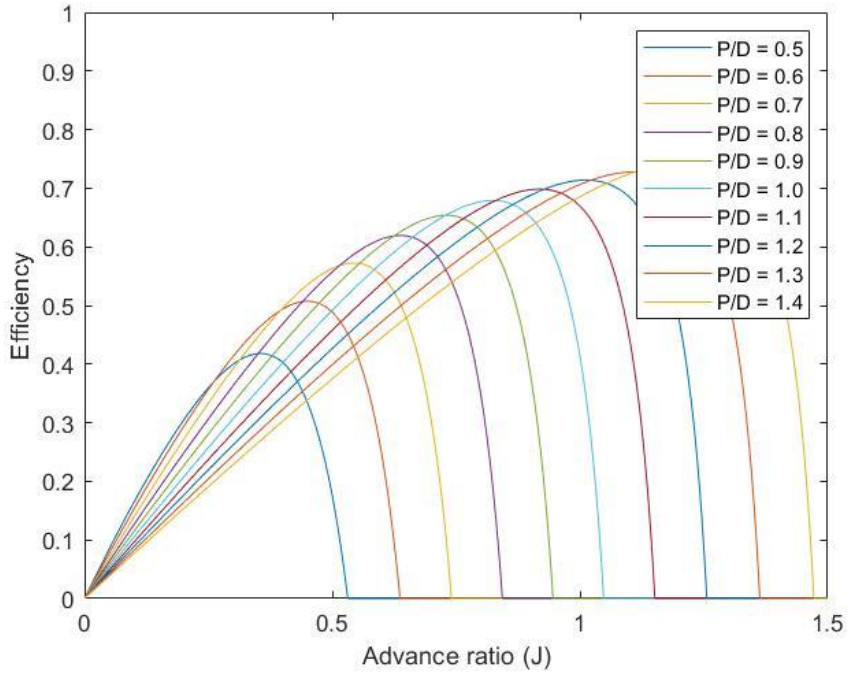

Figure 9) Wageningen B-series 4-blade propeller open-water efficiencies with varying P/D-ratios. Computed using MATLAB-code in appendix 2 with imported data from appendix 1 using eq (28), (31) and (32).

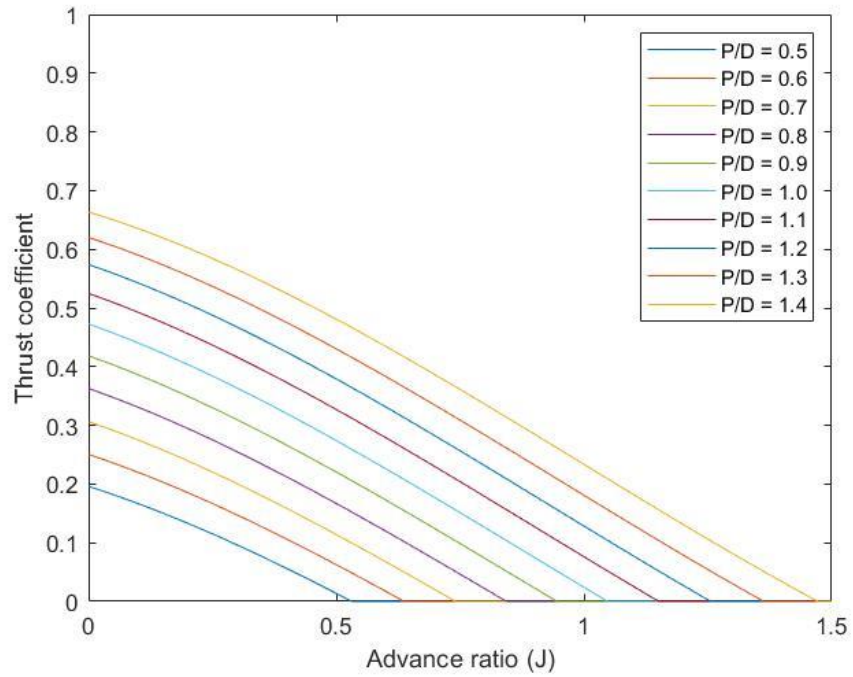

Figure 10) Wageningen B-series 4-blade propeller thrust coefficients with varying P/D-ratios. Computed using MATLAB-code in appendix 2 with imported data from appendix 1 using eq. (28), (31) and (32).

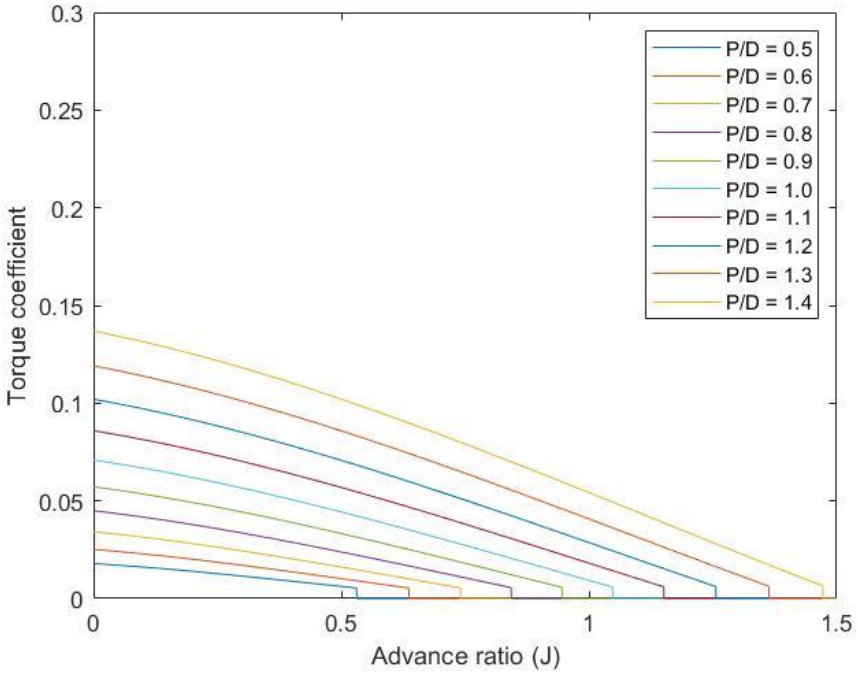

Figure 11) Wageningen B-series 4-blade propeller torque coefficients with varying P/D-ratios. Computed using MATLAB-code in appendix 2 with imported data from appendix 1 using eq (28), (31) and (32).

The increase of propeller diameter in the Holtrop-Mennen method has the tendency to lower the thrust deduction factor and have a minor impact on the wake fraction and hull efficiency.

Figure 12 shows the impact of the increase in propeller diameter on a 144 m meter long vessel. The Computation has been made with MATLAB codes found in appendixes 2 and 3. The only difference in calculations have been the increase of propeller diameter by 0.6 m, all other parameters have been unchanged.

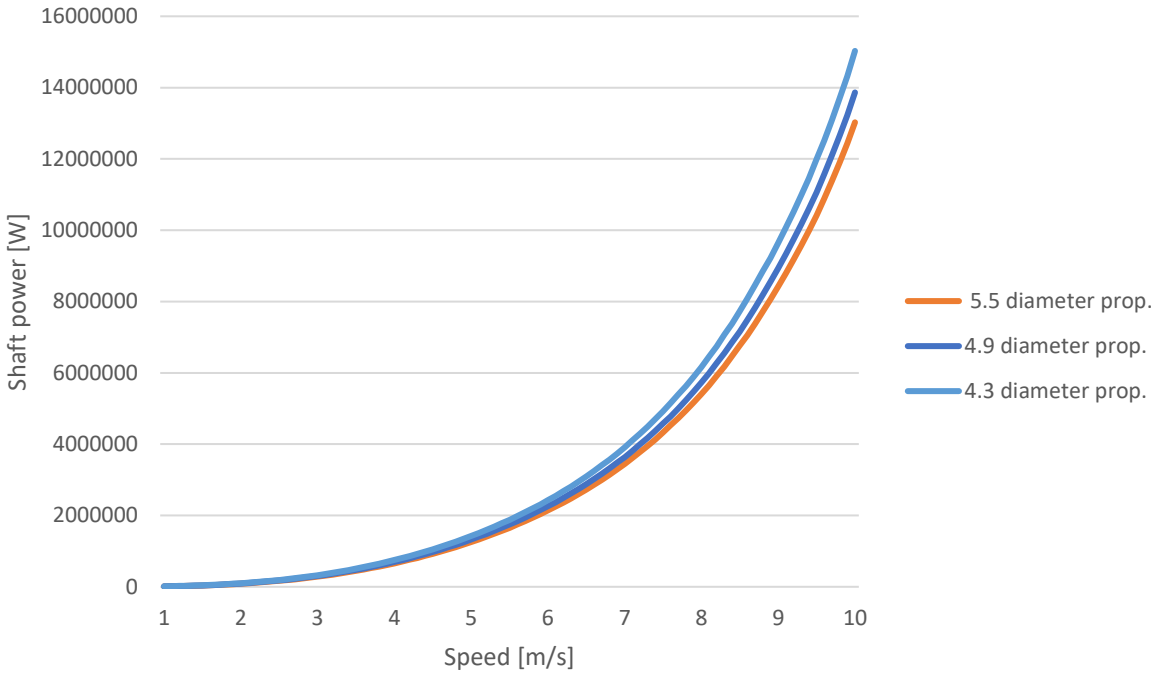

Figure 12) Effects of propeller diameter increase on propeller efficiency. Computed with Matlab code in Appendixes 2 and 3.

A significant amount of losses generated by the propeller is the inefficiency of rotating waterflow the propeller generates. These losses can be subdued by using a counter-rotating propeller (referred to CRP later in the text). The CRP consists of a pair of propellers rotating in opposite directions on the same propulsion shaft. According to [29], the losses caused by the rotating exit flow represent 8-10% of total propeller losses, and that a well-designed CRP-system can decrease the total power required to propel the ship with constant velocity compared to a similar ship with a conventional propeller by up to 6 %. [30] and [31] in their study show similar results in model tests and full-scale efficiency predictions. The negative factors on CRP-system are its mechanical complexity and price.

2.3 Electrical drives in marine applications and their efficiencies

In this chapter the existing technologies within the marine industry covering the electrical generating sets (referred as gensets from now on in this paper), shaft generators and electrical propulsion technologies and their efficiencies are reviewed in short. A brief insight in marine electrical installations and design is also discussed. Installations and design in this work consists of discussion about electrical network design and electrical machine configurations used in the industry. Finally, the chapter also holds a short listing of some manufacturers of electric machines within the maritime industry.

2.3.1 Marine electrical network

Installations and marine electrical network design are governed by the classification societies. A classification society can be considered as an external evaluation organization for safety and design of a ship. Although classification societies also evaluate subjects within land-based and offshore industry, they are best known for maritime evaluation operation. The rules and standards of classification societies exist because the technical rules and standards of the flag state of the ship, generally do not apply to ships in international traffic, therefore an external evaluator whose jurisdiction does not end at national borders has redeemed necessary.

The classification society rules governing electrical installation and network design include design rules and principles, such as the type of the electrical network, voltage, frequency, total harmonic distortion and their total deviation from base values. And technical rules to factors as for example: the choice and dimensioning of cables, operating curves and limits of generator breakers and circuit breakers.

The ships electrical distribution network according to classification society *Det Norske Veritas* (DNV) [32] can be of following types:
AC-grids:

1. three-phase three-wire with high-resistance earthed neutral
2. three-phase three-wire with low-resistance earthed neutral
3. three-phase three-wire with directly earthed neutral
4. three-phase three-wire with insulated neutral.
5. three-phase four-wire with neutral earthed, but without hull return (<500V)

6. single-phase two-wire with insulated neutral (<500V)
7. single-phase two wire with one phase earthed at the power source, but without hull return. (<500V)

DC-grids:

1. two-wire insulated
2. two-wire with one pole earthed at the power source (without hull return)
3. single-wire with hull return (only in special cases)

DC-grids onboard ships are usually low-voltage systems for battery backed-up fail redundant critical systems. These include systems such as: navigational equipment, control equipment for propulsion and power generation, safety equipment, emergency lighting, etc. Whereas AC-grids usually feed all other high-power consumers, such as: lighting, heating, cooking equipment, electric motors and drives, pumps, cargo handling equipment, hand-held appliances, propulsion in electric propulsion, etc. The most common distribution network type is an insulated network type, or IT-network.

In an IT-type network the power to the consumer is always taken between two phases, different voltage levels are acquired by a transformer. As opposed to a land-based system, TN-S, the power to a handheld 230 VAC appliance is taken between a phase and neutral, in an IT-system the power comes between two phases. The power is generated at a higher voltage (smaller vessels 400 V) and then reduced to lower levels via a transformer to suit the needs of the consumer [33]. Practically all naval vessels in Finland utilize this type of network.

The Source of main electrical power is a usually a mechanically driven generator composed from, most commonly a diesel engine and a generator. Gas turbine driven generators are almost exclusively found on larger navy vessels, for example *Flight IIA Arleigh Burke-class* destroyers use 3 *Rolls-Royce* AG9140 gas turbine-generating sets per ship [34]. Although diesel gensets are most common source of electrical power, classification society rules allow the main source of power to be a static device such as a fuel cell [32]. According to the classification society rules, the electrical network onboard has to redundant on a component level. In essence this means that a fault in any of the components shall not affect the basic operation of the ship [32].

An electric machine onboard a ship can practically be of any type, as long it complies with classification society rules. Permanent magnet machines have additional general and redundancy requirements, these are found in [32] section 5.3. As a motor in the small power range the most common is the squirrel-cage asynchronous motor, and as a power generator, an electrically excited synchronous machine is the most common.

2.3.2 Gensets

Several marine diesel engine manufacturers provide ready engineered gensets using in-house diesel engine and a third party manufactured electrical generator as a “bolt-on” installation. The generating set consists usually of a medium-speed or high-speed, category II or III diesel engine, an electrical generator, a baseplate, and an electronic engine governing system. The efficiency of the generator in a genset is quite high, typically between 0.95 – 0.97 [18] [35] [36].

Practically, every marine diesel engine can be engineered to work as a genset, the prime power source for the genset is a diesel engine working either with marine diesel, heavy fuel oil or liquified natural gas. The number of engine manufacturers for marine gensets is considerably fewer than the number of manufacturers for electrical generators, in the power range above 1 MW some of the most common genset manufacturers are:

Wärtsilä

Arguably the market leader in marine engines in installed power in medium and low speed engines globally, Wärtsilä has a substantial portfolio of gensets in marine traffic and land-based power plants. Figure 13 illustrates Wärtsilä’s diesel genset portfolio. The first number prior to the letter L or V, indicates the number of cylinders in the engine, the letter L or V the configuration of the engine (L for inline or V for V-cylinder configuration), the number after engine configuration is the bore of the cylinders in centimeters.

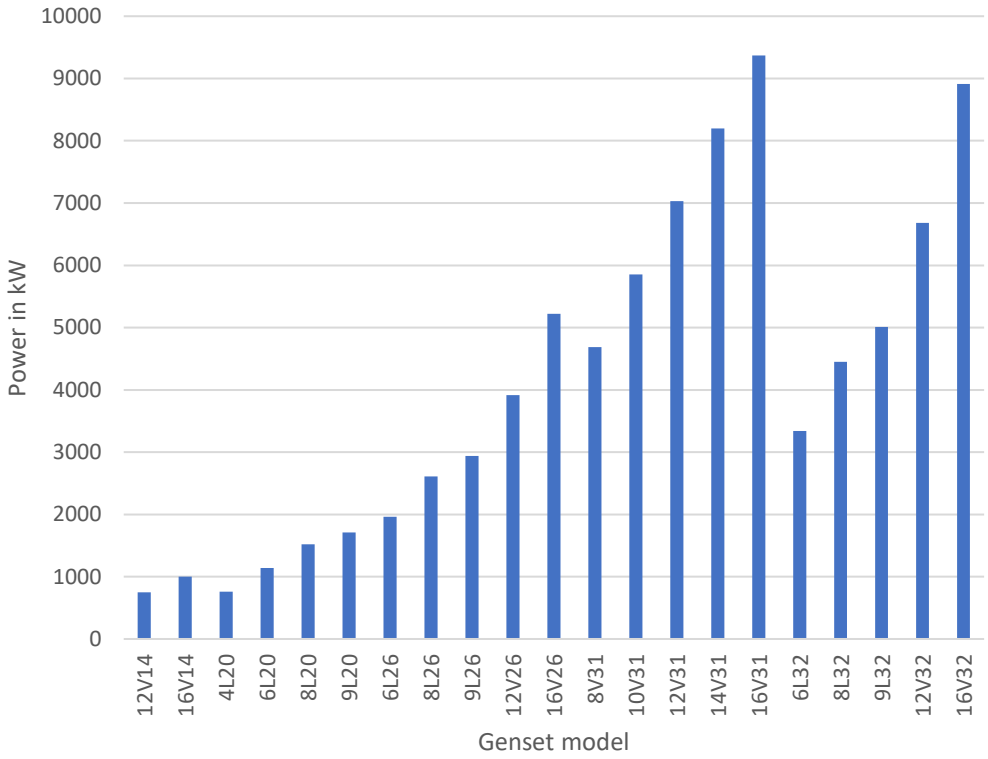

Figure 13) Wärtsilä genset product range [26].

MTU Friedrichshafen

MTU (*Motoren und Turbinen union)* genset range consists of 8-, 12- and 16-cylinder versions of 4000-series fast diesel engines, with peak power reaching 2.100 kVA. Reported generator efficiency is 0.96 and power factor 0.8. [37]

Caterpillar/MaK

Caterpillar holds the brands Cat and Mak that produce marine gensets. Cat genset range starts with the C32 model, with a maximum power rating of 1.175 kVA, ending to C280-16 with 6.050 kVA. MaK gensets are larger, their power range ends with the 16-cylinder VM46DF genset producing 18.528 kVA. [38]

MAN diesel

MAN diesel has a wide range of marine gensets starting from <1.000 kVA gensets to the biggest, the 172 ton 20-cylinder MAN V32/44CR genset. [18]

Rolls-royce

Rolls-Royce (after 2019 sold by Kongsberg Marine) holds the Bergen-series of marine engines premanufactured to a range of marine gensets of C25:33L and B33:45L for liquid fuel and Bergen C26:33L and B36:45 for gas fuels. [39]

2.3.3 Shaft generators

Shaft generators can be divided into two categories:

1. Shaft generators driven by a gearbox
2. Shaft generators driven by the propulsion shaft itself.

The fundamental difference between these two types of electric machines is their rotational speed. The gearbox driven units usually operate at a significantly higher rotational speed than the units placed directly on the propulsion shaft. Since the propulsion shaft has a relatively low rotational speed due to the natural behavior of the propeller (rotational speeds usually in the range 60-200 RPM), the shaft mounted generator must either have high number of poles or the frequency must be increased by a frequency converter to match the frequency of the network.

Notable is that an electric machine is a versatile component, many machines can be used as a genset generator or as a gearbox driven shaft generator without any notable modifications. There are a vast number of manufacturers of marine generators that can be used as shaft generators, some listed below:

ABB

ABB offers gearbox driven shaft generators in a modular and standard series, both starting in frame size 400 with the largest frame size of 450 for the standard series and 630 for the modular series. Power range for the modular series generators go up to 5000 kVA at rated power factor of 0.8. ABB also offers shaft driven generators with an “off the shelf” solution to add a variable speed converter to the generator and energy storage to achieve redundant “take me home”- emergency operating mode and hybrid mode to the vessel. [40]

VEM motors

VEM motors offers gearbox operated shaft generators in the output range of 500 – 30,000 kVA with pole number by choice from 4 to 14 pole machine, and shaft installed generators up to 7,500 kVA with maximum pole number of 24 poles. [41]

GE electric

GE makes electric generators and shaft generators for industrial and marine installations. Marine portfolio consists of “Beta” and “Delta”-range, with both having pole number-range 6 to 22 pole machines. Power range for “Beta” range machines is 5.000 – 20.000 kVA and 2.500 – 45.000 kVA for the “Delta”-range. GE shaft-mounted generator is designed to operate both in PTI and PTO modes and is always equipped with a frequency converter. [42] [43]

Cummins generator technologies

Cummins generator technologies hold two brands: Stamford generators and AvK alternators. Stamford generators are somewhat smaller than AvK alternators, Stamford power range starts with the P0- model and ends with the S9- model at 4,500 kVA. The AvK power range starts at 1,100 kVA and ends at 10,800 kVA. [44]

Nidec Motor Corporation

Nidec motor corp. holds the brands Leroy-Somer and Kato engineering that provide marine alternators up to 35 MW to be used either at gearbox operated or as a part of a genset.

WEG Electric

WEG Electric offers marine generators in three frame sizes 450, 500 and 560, all being 4-pole machines, with the output range starting from 1,100 to 3,000 kVA. [45]

ATB Austria Antriebstechnik

ATB manufacturers 4 pole synchronous up to 10 MW with frame sizes up to 1700. ATB also offer asynchronous generators with same power ratings but with more pole alternatives than with synchronous generators. [46]

Brush Group

Brush group manufactures large, mainly gas and steam turbine driven generators for wide range of purposes, also marine applications. Power range for four pole air cooled generators start from 10 MVA ending to 65 MVA, two pole machines having a power range all the way up to 350 MVA. [47]

Lloyd Dynamowerke (LDW)

LDW offer synchronous generators for shipbuilding industry in power range of 4.000 – 65.000 kVA, with synchronous speed at various rpm configurations. [48]

Marelli Motori Group

Marelli motori group manufactures five types of marine generators; MJHRM-, MJRM-, MJHM-, MJBM- and MJVM-types of machines. All of these can be ordered varying from 4 to 12 poles, with the largest frame sizes being 1.250. power range reaches its peak at 11.000 kVA. [49]

Mecc Alte SpA

Mecc Alte manufactures marine alternators up to nominal power of 2.500 kVA in low voltage applications only. Industrial alternator range is substantially wider, covering wider voltage and pole options. [50]

2.3.4 Electric propulsion

Electric propulsion in this work is defined as a propulsion system in which the prime mover of the vessel is an electric motor instead of a marine diesel engine. The diesel-electric drivetrain is quite an old invention. The first diesel-electric vessels were built about 120 years ago, and e.g., the largest warships in Finland, the *Väinämöinen*-class coastal battleships were electrically driven. The electric propulsion systems can be divided into two categories; an electric motor driving a fixed pitch propeller by a shaft from inside the ship's hull, or a rudder propeller system where the electric motor is in the hub itself. Electric propulsion, and especially the podded type of electric propulsion is increasing in popularity, particularly among cruise vessels. For example, the Oasis-class cruise ships are equipped with ABB commissioned Azipod-propulsion system containing three 20 MW electric pod units.

The Azipod type propulsion system has several advantages that explain why these kinds of systems are becoming more popular. According to ABB, some of these advantages are:

- Design flexibility. Since the propulsion unit needs no long shaft lines, the engine room layout can be designed more compact and economical in space.
- Maneuverability. On a conventional rudder, the steering force on a ship is dependent on the flow of water along the rudder surface, which at low maneuver speeds is

compromised on a conventional system. But with a podded system the steering force is diverted to a certain direction, making a stern tunnel thruster pointless.

- Improved safety. Improved safety due to more maneuverable ship lowers the risk for accidents. Especially in bad weather.
- Fuel economy. The podded drivetrain system is more economical due to the increased hydrodynamical efficiency of the ship's hull. The construction of the podded propulsion system enables the waterflow to the propeller on a podded propulsion system to be less disturbed and therefore less turbulent on the propeller blade, also the absence of driveshafts and their brackets, the aft of the ship can be designed more streamlined thus lowering the wake fraction. The effect of turbulence caused by the shafts and shaft brackets can be visualized in figure 14. Previously mentioned factors combined, ABB claims the Azipod system to have 12% better overall efficiency compared to a conventionally driven system at a speed of 22 knots in delivered power. [51]

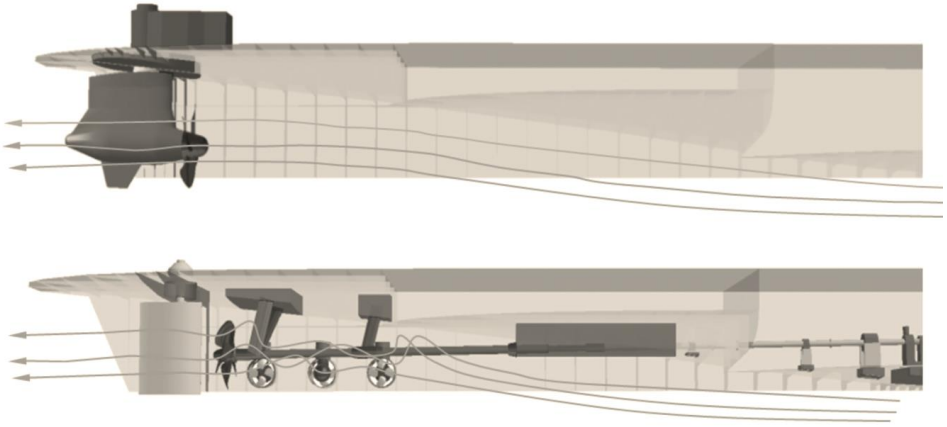

Figure 14) Waterflow around a Podded propulsion system and a conventional shafted system [41].

- Economical in payload. Since the design flexibility is increased, and engine room takes less space, that space can be utilized by the company to increase its cargo capacity, thus increasing total revenue.

Ice braking capabilities. The podded drivetrain system enables the double acting ship concept, where the ship moves ahead in normal sea conditions but turns to move astern in heavy ice conditions using the Azipod to crush ice with the propellers.

Figure 15 shows a computation with the Holtrop-Mennen method calculator in appendix 3 of a ship with altered hull form and parameters to suit a Azipod driven ship. The calculation

utilizes the same 144 m long vessel with a 5.5-meter FP-propeller in figure 12. The parameters altered in the computation are listed in table 4:

Table 4) Parameters for computations for the Azipod driven vessel and the shaft driven vessel.

Azipod vessel			Shaft driven vessel		
C_stern	=	-25	C_stern	=	0
C_b	=	0.62	C_b	=	0.6452
S_app	=	[0]	S_app	=	[52 26 3 0.75]
k2	=	[0]	k2	=	[0.4 3 1 1]

The parameters are all related to the aft structure of the ship. The parameter *C_stern* is the parameter built in the Holtrop-Mennen method to picture the shape of the aft, in this case, the value -*25* is correction factor to represent a flat and streamlined hull shape in the aft, the value zero is the correction factor for a normal aft shape. The parameter *C_b* (block coefficient of the vessel) has been slightly reduced to match the alterations in aft structure of the vessel. The parameters *S_app* and *k2*, are the matrixes required for the resistance calculations of the residuary resistance component. The first index of the matrix *S_app* in the shaft driven vessel is the bilge keel of the vessel, the second index are the shaft brackets, the third is the exposed shaft itself and the fourth is a skeg. All of the residuary matrix values have been removed for the Azipod vessel as they would be absent on real ship of this type.

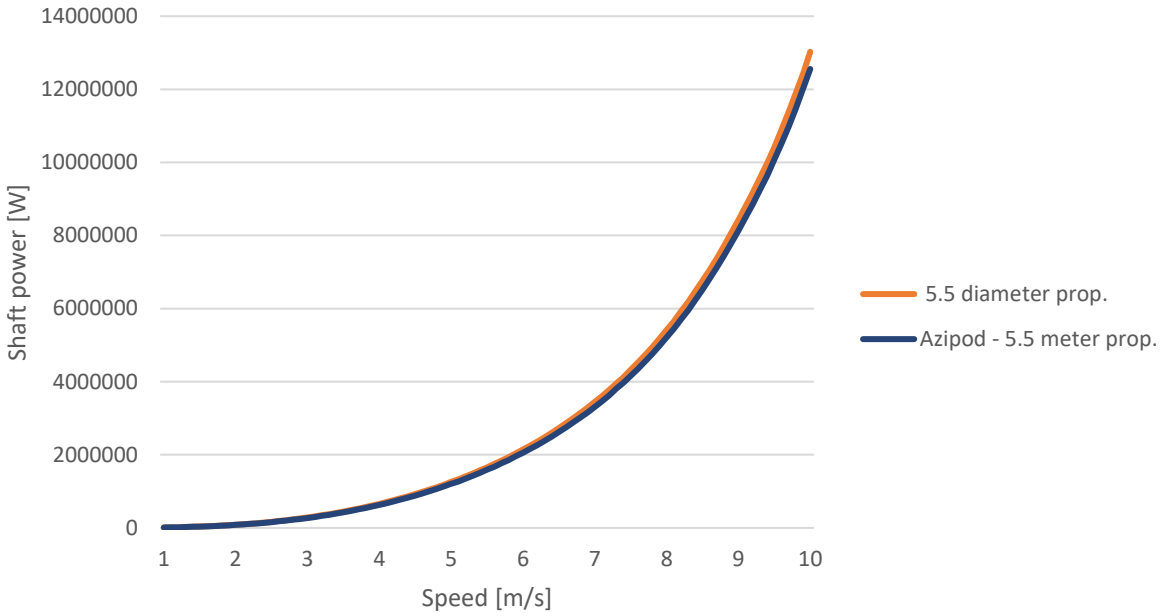

Figure 15) Comparison between a Azipod vessel and a conventional vessel in propulsive efficiency. Computed with appendix 3.

Figure 15 shows the results of the computation described above, the reduction in power with the same speed and parameters excluding the parameters listed in table 5 with maximum speed is 0.47 MW, which represents a 3.6 % decrease in power compared to the conventional ship. Although the computation show an efficiency increase, the computed increase is somewhat lower than marketed by ABB. One has to keep in mind that the Holtrop-Mennen method was not originally intended for calculations for an Azipod system, and therefore cannot be fully reliable.

The lowered turbulence also has a great impact on the noise generated by the propulsion system. The turbulence caused by the propeller shaft lines, shaft brackets and ship's hull are non-existent in a podded system. Also, since the propeller can be considered to have been mounted on the rudder, the noise of water hitting and changing its direction on the rudder of a conventional ship is basically neglected. This could be very beneficial for example naval ships operating in a mined area when acoustic signature of the ship needs be kept at a minimum, given that the pod system could be fitted with an internal degaussing system to prevent the magnetic signature from compromising the ship. Together with a battery storage

system, the vessel could in theory operate short periods of time with practically neglectable acoustic signature.

The electric motor type in an electric propulsion system in generally either an externally excited synchronous motor, permanent magnet synchronous motor or an induction motor. An Azipod system utilize on either one of these [52]. The permanent magnet Azipod electric motor has an efficiency rating of 98 %, the induction version is at 96% efficiency [53]. In 2017 ABB achieved a 99 % efficiency with a 6-pole 44MW synchronous motor, when typical efficiencies on motors of this type is between 98.2 and 98.8 % [54].

2.3.5 Drives in marine propulsion

The drives in marine propulsion motors are generally even more efficient than the motor they drive. ABB states that the ACS6080 marine drive has an efficiency of >99 %, Nidec Corporation Silconvert FH drive is marketed at 98 % efficiency. Both drives are medium voltage drives, the Siloconvert has a maximum voltage of 6.6 kV and the ACS6080 a maximum voltage of 3.3 kV. The ACS6080 is has a 6-, 12- or 24 pulse diode rectifier and is rated for permanent magnet, induction and synchronous motors. The Slioconvert utilizes IGBT power transistors and can operate in 4 quadrants. [55] [56]

3 FUEL EFFICIENCY CALCULATIONS

The calculations in this chapter are based on Wageningen B-series propeller polynomials, the Holtrop-Mennen resistance prediction method and ITTC78 power prediction method. All the above mentioned are calculated using Matlab-calculators found in appendixes 2,3 and 4. The polynomials for propeller calculation can be found in appendix 1. The powertrain efficiency is calculated using eq. (4) and (5).

Fuel consumption calculations are based on the speed of the vessel. Data originate from Automatic Identification System (AIS) collected from www.vesselfinder.com. The AIS is a system used mainly by ships and Vessel Traffic Service (VTS) centers to identify and locate ships. AIS provides ships with a means to electronically exchange vessel information such as identification, position, heading, and speed with nearby ships and VTS centers. This information is displayed on the device's own or ECDIS display. AIS is intended to assist ship's officers and enable maritime authorities to track and monitor the movements of ships.

With the AIS-data, the vessel speed is then converted into propulsion engine load. For the calculations, the technical specifications of the vessel are required. These specifications are collected from open-source information for the specific vessel from which the AIS-data has been collected. The vessels under research are vessels that exist and operate in various sea areas. If the information is not received otherwise, the specification in question is estimated, using publications within the maritime industry. The hotel load (i.e., the electrical consumption by all users) is estimated roughly, with hotel loads being estimated to be largest in maneuvering situations due to transverse thrusters.

The AIS data is delivered in CSV-format, from which the data have been converted into excel-worksheet and consequently into a column vector in Matlab using the *import data*-tool. The hotel load is estimated using either rough estimate collected from the vessel itself in hand or estimated from literature. The hotel load is generated into an equally long excel-column as the speed vector collected from AIS-data. Into the hotel load, some ripple in electrical load has been added to represent the random nature of the load in real life. The ripple is generated using excel-function *rand*. To each port exit and enter, the hotel load is increased to represent the transverse thruster of the vessel.

The calculations require the BSFC-value for both main engines and auxiliary engines as well as the SFC-map for both engines. In this thesis only one SFC-map is used, the map in question is the map found in table 3, as it represents a typical SFC-map of a diesel engine. The SFC-values in table 3 are PU-values, scaled with BSFC-values. In table 3, the rows represent the PU rotational speed of the engine and columns the torque of the engine in PU. Propeller rotational speed, obtained from the code in appendix 3, is scaled to PU-rotational value, and power with the rotational speed is scaled to PU-torque. With the known torque and rotational speed PU-values, the SFC-value for that single operating point is acquired by calculating the factor of BSFC-value and its corresponding SFC PU-value from table 3. In operational mode 3, the PU-rotational speed of the engine is fixed to row 7, to represent the constant synchronous speed of the engine.

The dataset acquired has a datapoint interval of 5 minutes, the load is assumed to be constant within these five minutes of observation. The operating modes 1, 2 and 3 in the calculator are different machinery setups. The Matlab-codes in appendixes 2,3 and 4 return variables *fuel_propulsion* and *fuel_generator*, these variables represent the fuel consumed over the entire period of observation at hand with given parameters.

Operating mode 1 is a conventional ship with main engines using either one or two propeller shafts, the auxiliary engines are added automatically by the calculator to ensure sufficient electrical balance. The auxiliary engines always have a 20 % reserve in power, if the power reserve drops below 20%, an additional auxiliary engine is coupled online.

Operating mode 2 is the shaft generator mode, whenever the main engine is rotating with 70% nominal speed and the increase in torque to the main engine does not overload the engine, the shaft generator is coupled on, and hotel load is transferred over to the shaft generator. Outside of the shaft generator synchronous operating speed the auxiliary engines behave like in operating mode 1.

Operating mode 3 is a diesel-electric mode, where all the propulsion power is transferred to the hotel load, the propulsion power is set to zero and all auxiliary engines behave like in operating mode 1. In essence, all the power onboard is labelled as hotel load, even if a part of the hotel load propellers the ship. The diesel electric propulsion in this spec is a shaft

driven propulsion system. An Azipod system can be modelled by using similar adjustments to ship parameters as listed in table 4.

3.1 Harbor tug

The harbor tug in question is a tug operating in southern Finland. The tug is a small vessel with a substantially light hotel-base load of 18 kW. The dataset for the tug is a sea trip from Hanko to Inkoo and back. The machinery best specific consumptions are estimated to be 191 g/kWh for main engines and 197 g/kWh for auxiliary engines. Typical for a harbor tug, the vessel has an over-dimensioned transverse thruster for its own purposes, 263 kW in power. Auxiliary engine peak power at normal hotel load generation is 200 kW and at electrical propulsion mode 500 kW and 197 g/kWh best specific consumption. Mechanical drivetrain efficiency is estimated at 0.94 and electric efficiency at 0.96. Figures 16 – 19 show the loads for the harbor tug in each operational mode according to computation with appendix 1, 2 and 3:

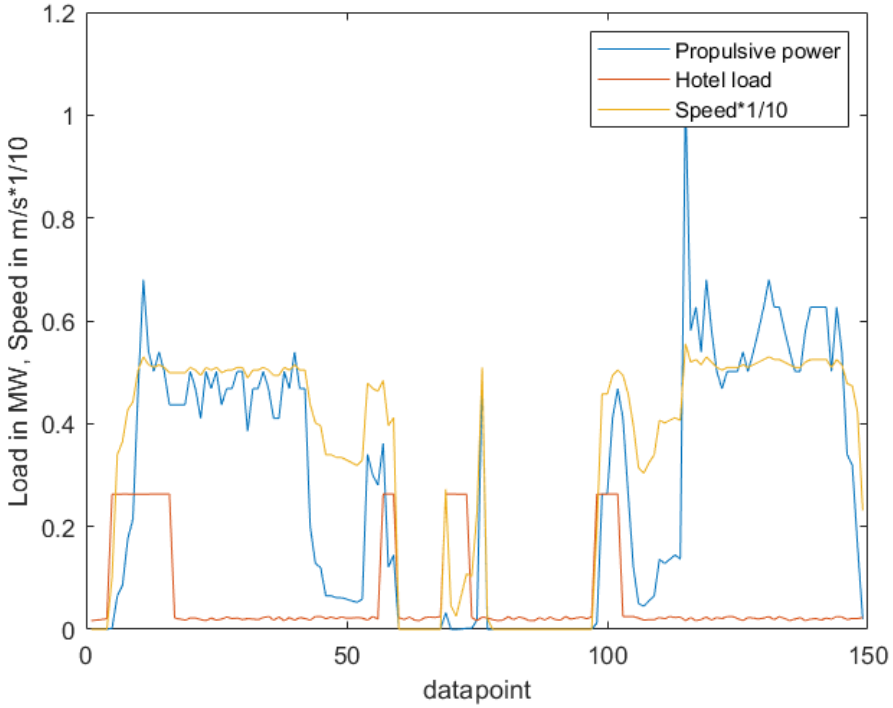

Figure 16) Speed- and load profiles of the harbor tug under analysis. Note the speed is illustrated in the figure as one tenth of the actual speed, factorization has been purely for graphical purposes only.

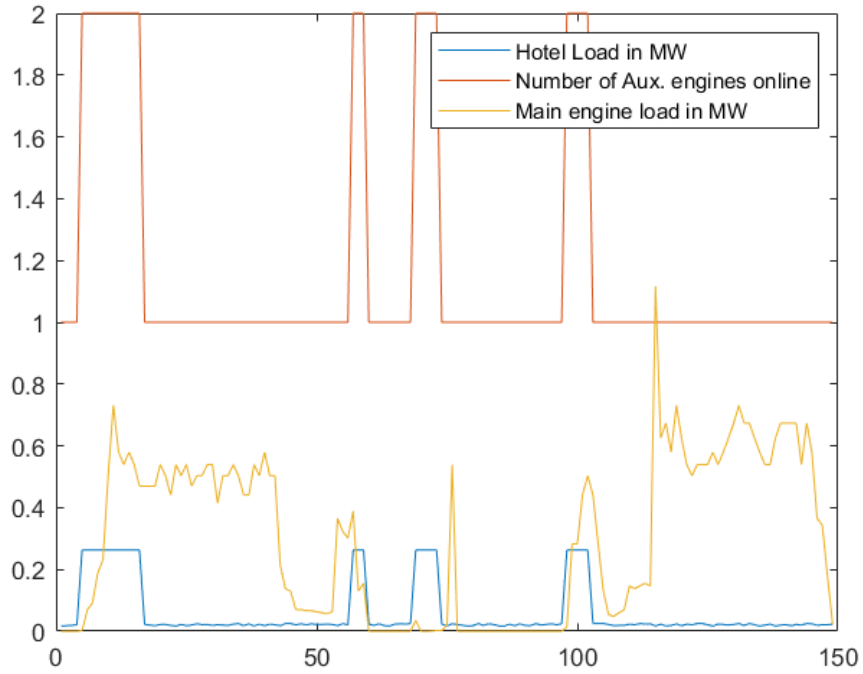

Figure 17) Harbor tug loads and auxiliary generator number in operational mode 1.

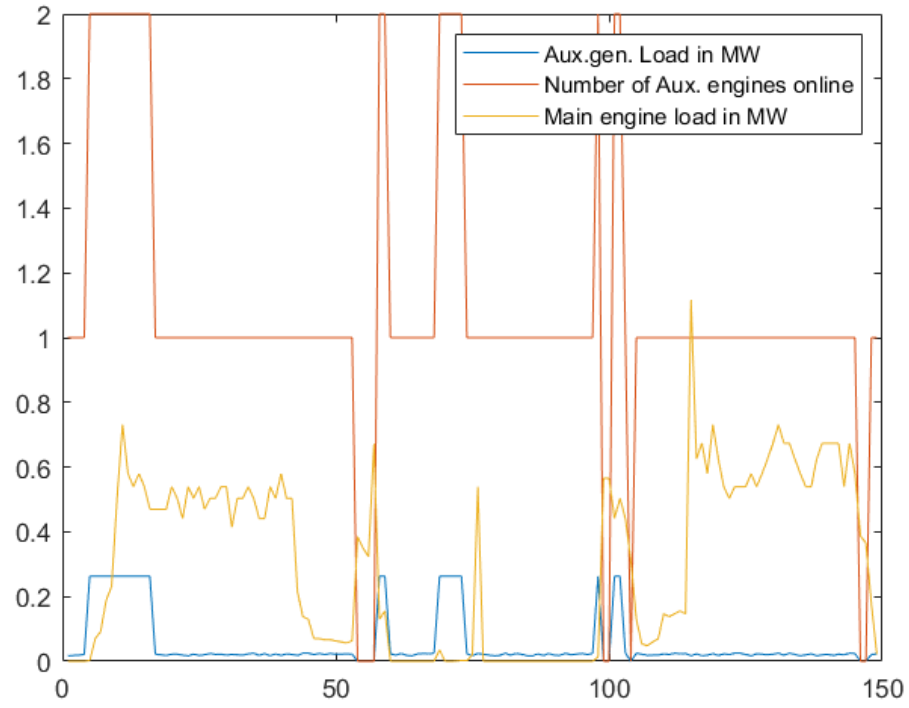

Figure 18) Harbor tug loads and auxiliary generator number in operational mode 2.

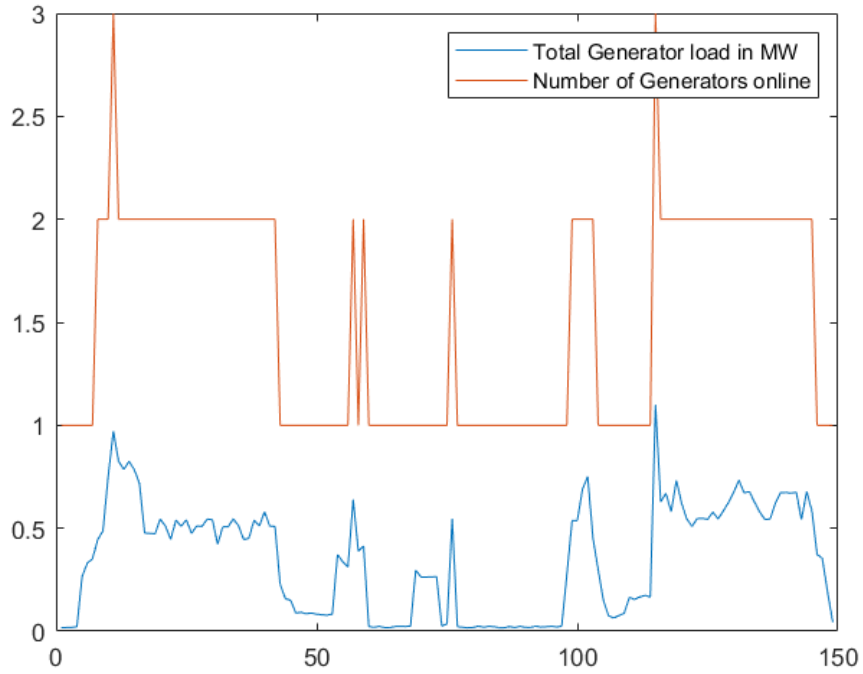

Figure 19) Harbor tug loads and generator number in operational mode 3.

When compared to figure 17, figure 18 shows only a few datapoints where the shaft generator is online. These points appear to be in situations where the power of the engine is at 0.4 – 0.5 of nominal power. Table 5 shows the fuel consumption for the harbor tug for each individual operational mode. The variables *fuel_propulsion* and *fuel_generator* are parameters obtainable from the code in appendix 3:

Table 5) Harbor tug fuel consumption for each operational mode.

	Fuel used[kg]		
	op. mode 1	op. mode 2	op. mode 3
fuel_propulsion	791	805	
fuel_generator	194	176	946
Total	985	981	946

3.2 Large containership

The containership under analysis is one of the largest ships in the world. The data consist of a journey between two ports in the Caribbean, one has to note that between datapoints 70 and 570 (a time period of roughly 8 hours) the vessel has been practically motionless, most likely waiting for port entry clearance. Therefore, the data itself is not ideal for any sort of calculations or analysis. This can be clearly viewed from figure 18. Best specific consumption is estimated for main engines 161 g/kWh and for auxiliary engines 180 g/kWh.

mechanical drivetrain efficiency estimated at 0.95 and electrical at 0.96. Generator power in mode 3 is set at 3 MW and peak efficiency at 170 g/kWh. Figures 20 – 23 shows the loads for the container ship in each operational mode according to computation with appendix 1,2 and 3:

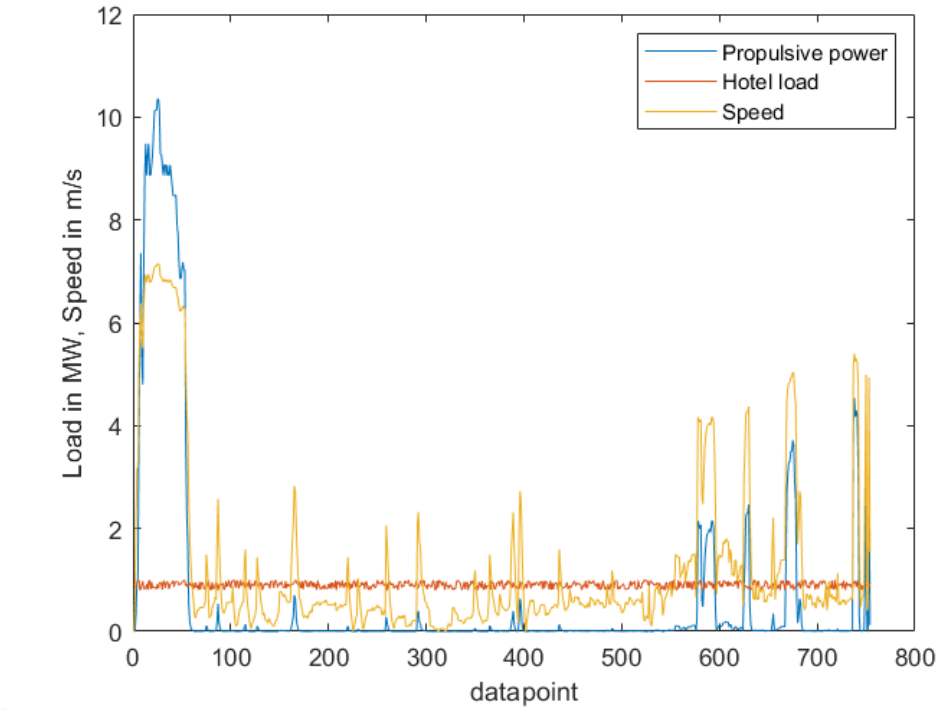

Figure 20) Speed- and load profiles of the containership under analysis.

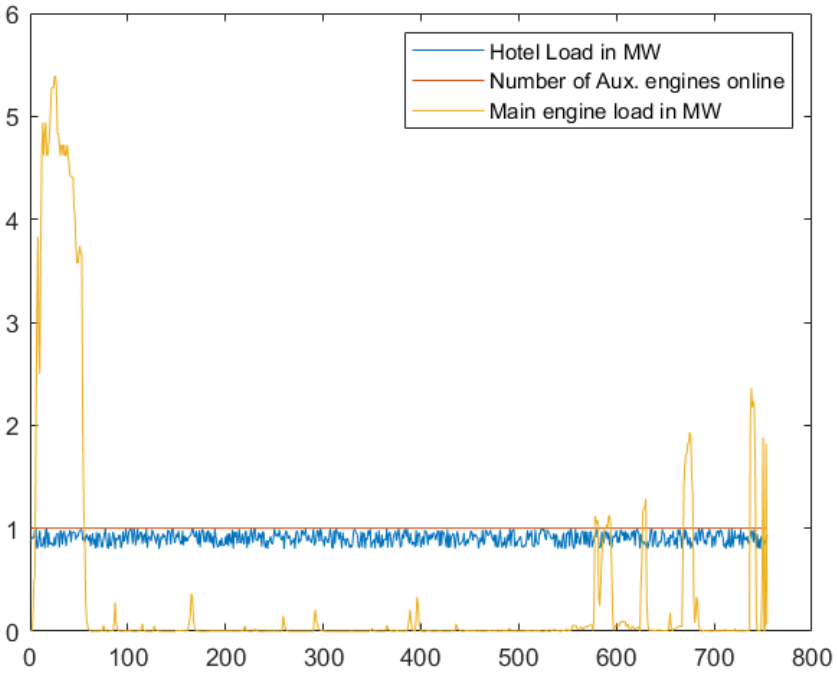

Figure 21) Container ship loads and auxiliary generator number in operational mode 1.

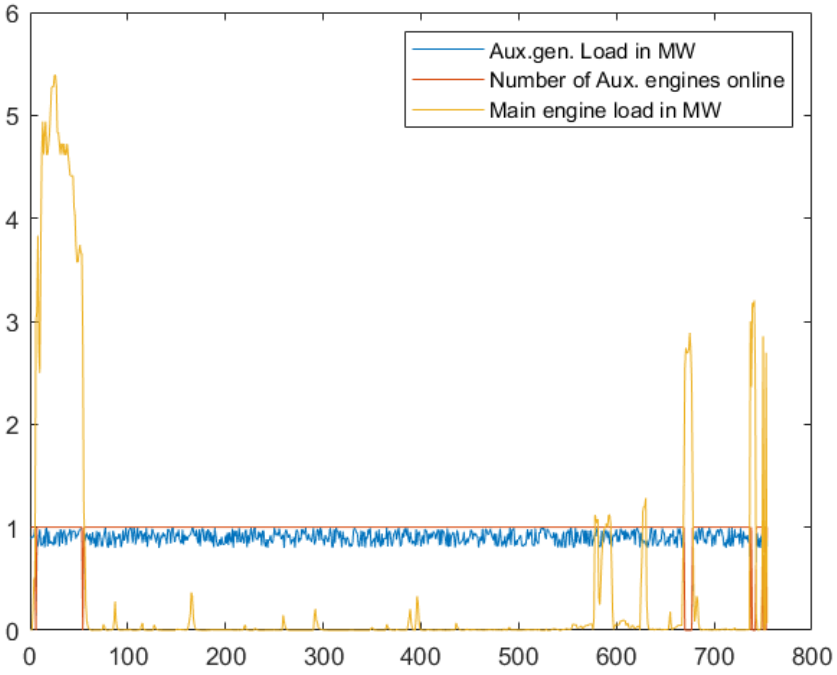

Figure 22) Container ship loads and auxiliary generator number in operational mode 2.

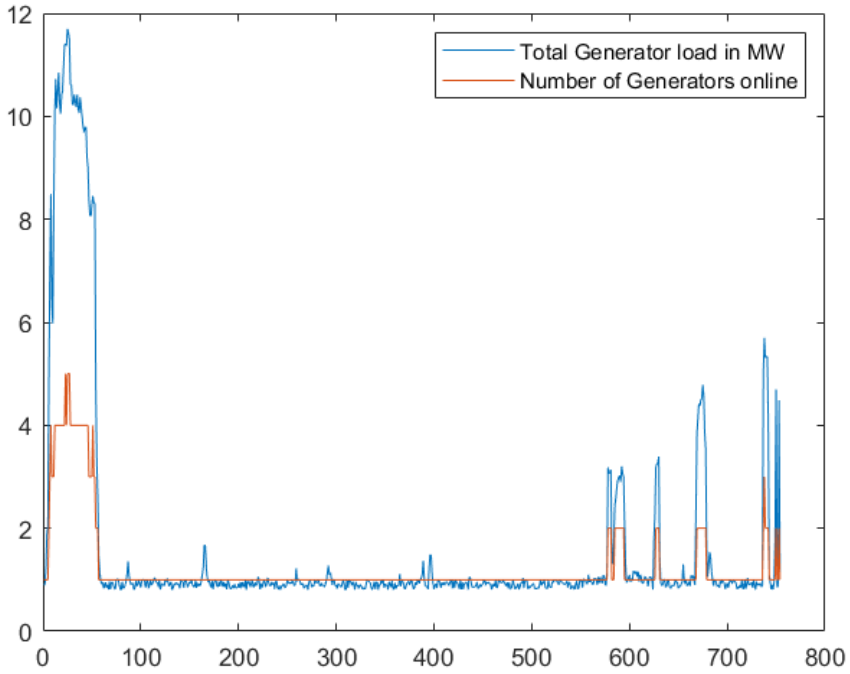

Figure 23) Container ship loads and generator number in operational mode 3.

Table 6 shows the fuel consumption for the containership for each individual operational mode:

Table 6)Containership fuel consumption for each operational mode.

	Fuel used[kg]		
	op. mode 1	op. mode 2	op. mode 3
fuel_generator	10994	10747	21277
fuel_propulsion	8804.07	9165	
Total	19798	19912	21277

3.3 Small bulk-cargo ship

The ship in question is a 155-meter-long vessel with an operating area in the Baltic Sea. The calculations require some initial assumptions, the main engine BSFC-value is assumed to be 166.0 g/kWh and auxiliary engine BSFC-value for 190.0, both matching to engines available for such a ship with a mechanical drivetrain efficiency of 0.96. For electrical operating mode, the BSFC-value is lowered to 170 g/kWh and an efficiency of 0.96 is estimated for the electrical drivetrain efficiency. Auxiliary engine peak power is set to 1.5 MW in modes 1 and 2, in electric mode the power is increased to 3 MW. Figures 24 – 27 shows the loads for the harbor tug in each operational mode according to computation with appendix 1, 2 and 3:

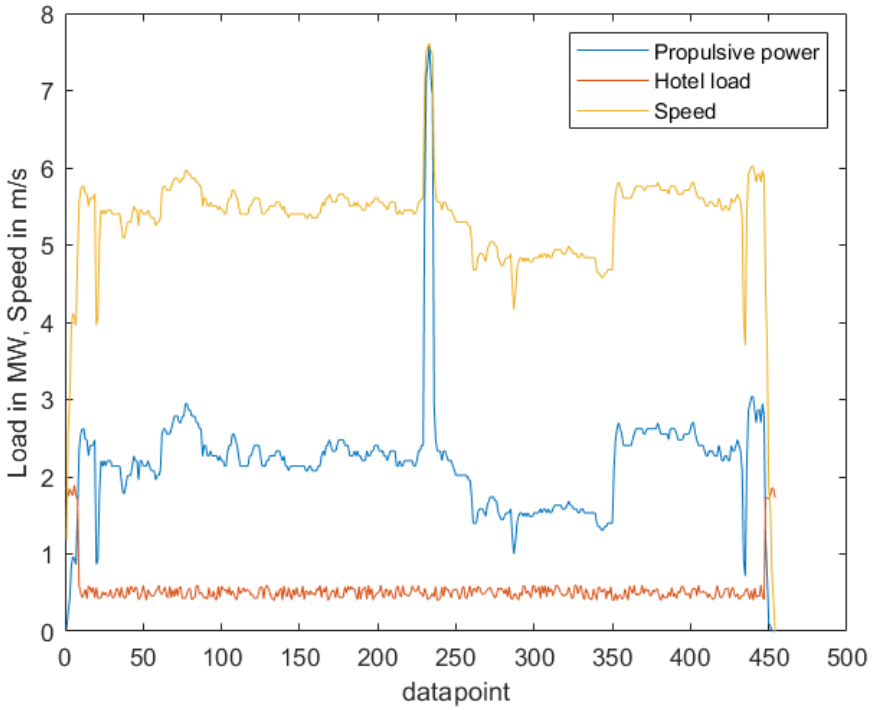

Figure 24) Speed- and load profiles of the bulk-cargo ship under analysis.

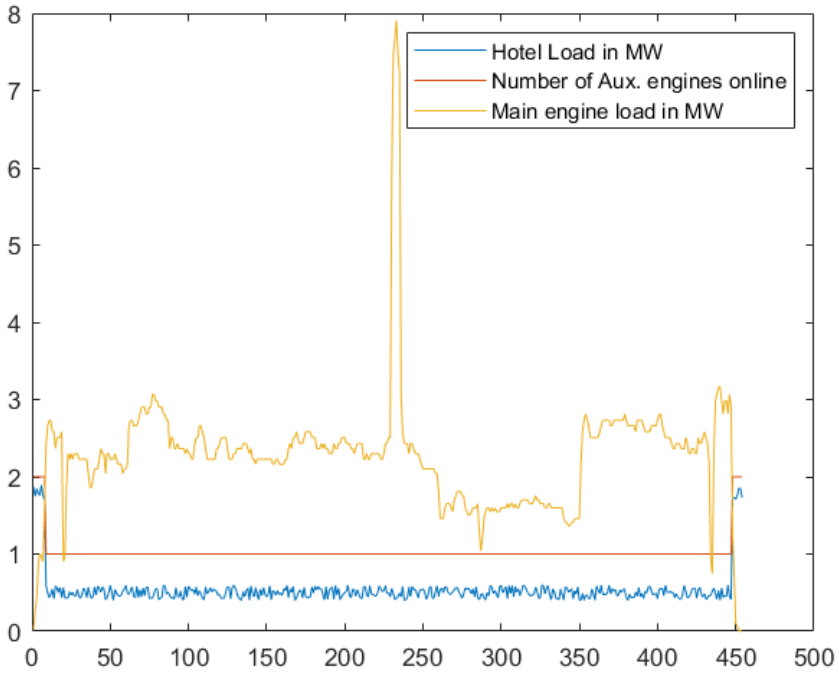

Figure 25) Bulk-cargo ship loads and auxiliary generator number in operational mode 1.

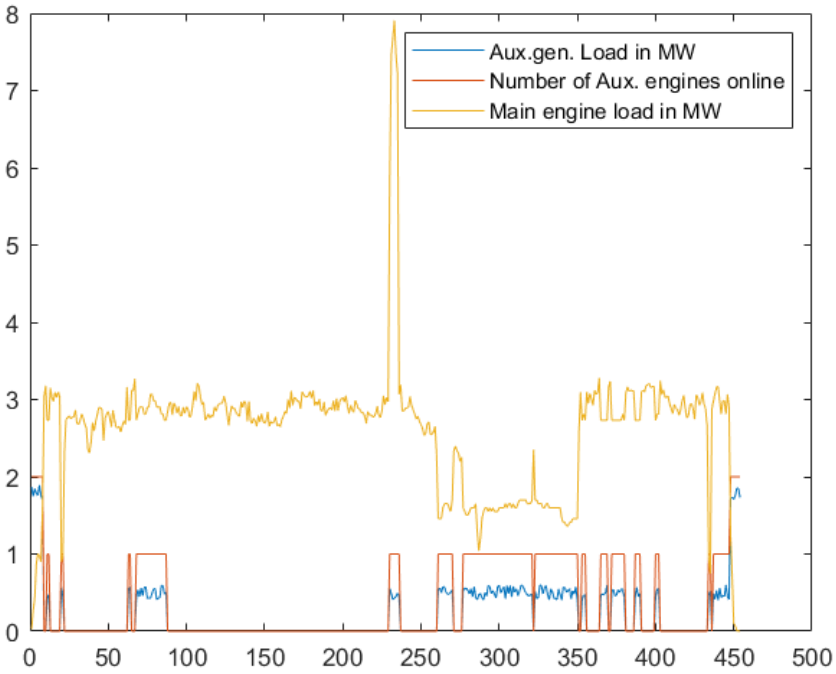

Figure 26) Bulk-cargo ship loads and auxiliary generator number in operational mode 2.

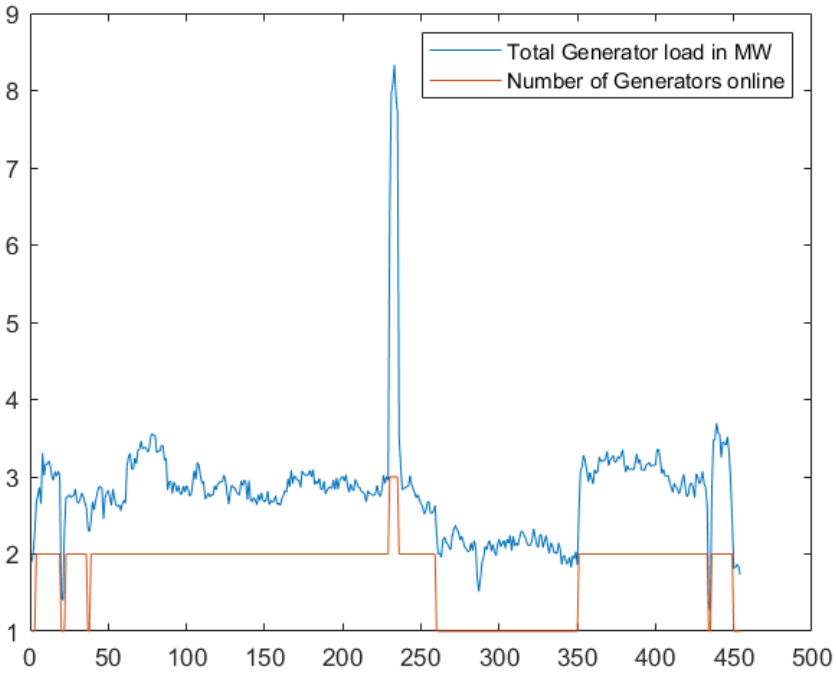

Figure 27) Bulk-cargo ship loads and generator number in operational mode 3.

Figure 26 show a clearly that the shaft generator has been online for several datapoint intervals over the period in question. This type of ship has traditionally biggest advantage of a shaft generator, the ship has long transitions at outer sea with practically constant main

engine load. The diesel-electric mode shows also significant fuel savings. Table 7 shows the fuel consumption for the bulk-cargo ship for each individual operational mode:

Table 7) Bulk-cargo ship fuel consumption for each operational mode.

	Fuel used[kg]		
	op. mode 1	op. mode 2	op. mode 3
fuel_propulsion	16332	18487	
fuel_generator	4423	1842	19802
Total	20756	20329	19802

3.4 Passenger ship

The passenger ship is a ship with a fixed route in the northern Baltic Sea. Main engine BSFC-value is 175 g/kWh and auxiliary engine BSFC-value is 180 g/kWh and peak power is 5 MW. Diesel electric operating mode is calculated using same auxiliary engine parameters as in modes 1 and 2, but with drivetrain efficiency of 0.96. mechanical drivetrain efficiency is estimated at 0.94. Figures 28 – 31 shows the loads for the harbor tug in each operational mode according to computation with appendix 1,2 and 3:

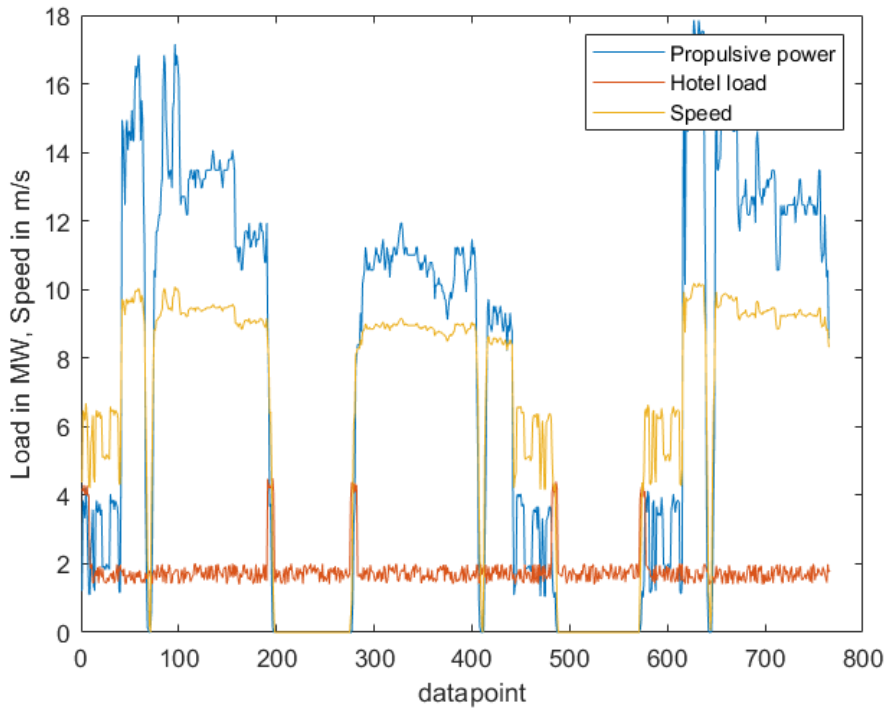

Figure 28) Speed- and load profiles of the passenger ship under analysis.

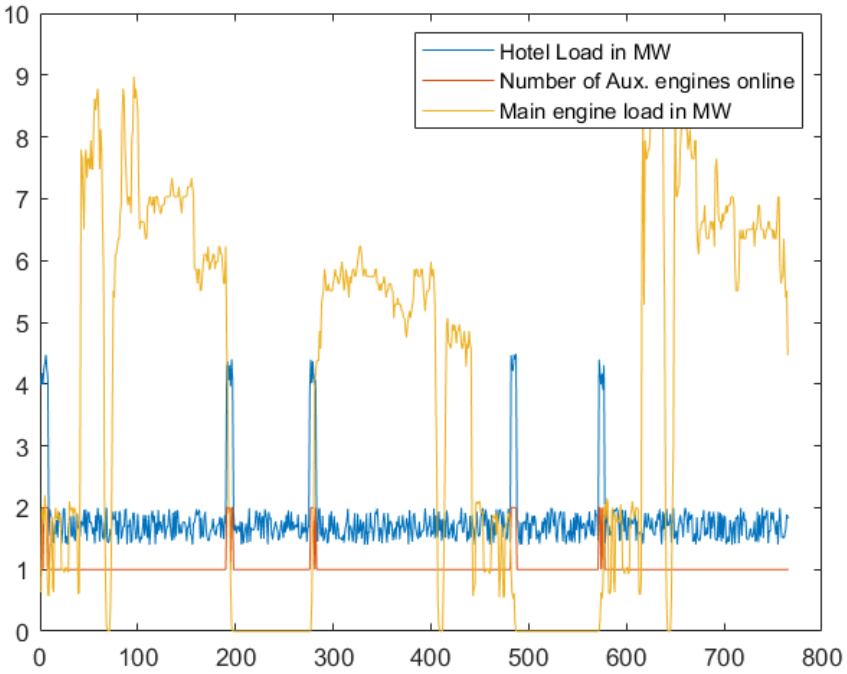

Figure 29) Passenger ship loads and auxiliary generator number in operational mode 1.

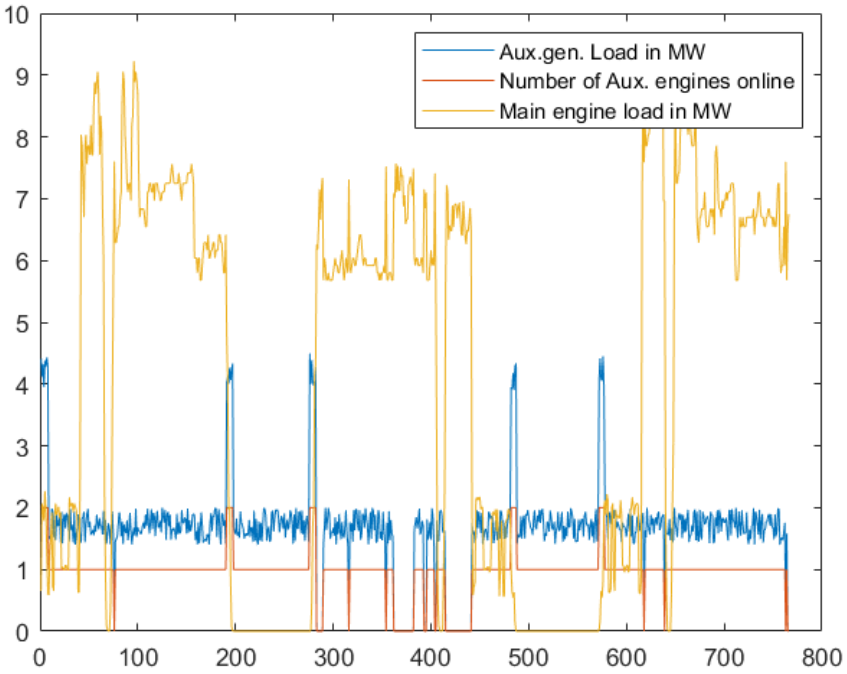

Figure 30) Passenger ship loads and auxiliary generator number in operational mode 2.

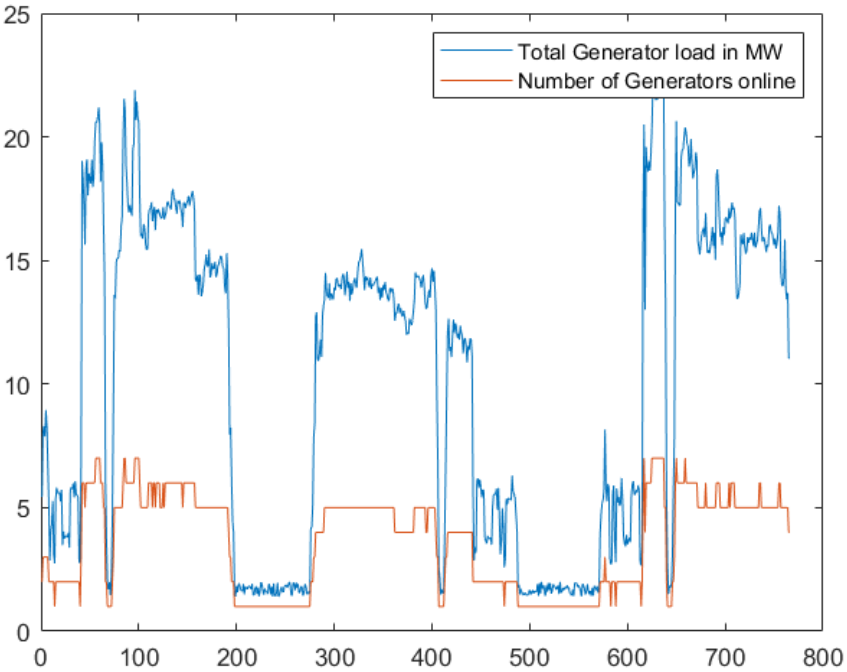

Figure 31) Passenger ship loads and generator number in operational mode 3.

As opposed to the bulk-cargo ship, the passenger ship has large variations in load over the dataset, and therefore as illustrated in figure 28, the shaft generator is only a few short moments online and thus saves no fuel. On the other hand, the diesel-electric mode appears to show quite substantial fuel savings. Table 8 shows the fuel consumption for the passenger ship for each individual operational mode:

Table 8) Passenger ship fuel consumption for each operational mode.

	Fuel used [kg]		
	op.mode 1	op.mode 2	op.mode 3
fuel_generator	23679	23559	112013
fuel_propulsion	91402	91588	
Total	115080	115146	112013

4 RESULTS

With responses to the inquiries to the shipbuilding industry, the questions predefined in chapter 1.3.1 can be answered:

- *"How is the total propulsion power estimation carried out in the design phase in shipbuilding?"*

- In the preliminary design phase, the earliest power estimate is based on reference ships, which drag is known from model and sea trials. By adjusting parameters on the newbuild, the earliest estimate is achieved. Later when the hull structure is known, the drag of the hull is calculated using RANS CFD-simulations. With the drag known, the efficiency of the propeller is added to calculations, and the required shaft power can be calculated. The efficiency of the propeller is based on series propellers, with the most notorious the Wageningen B series. [57] [7]

- *"What kind of operational requirements dictate the arrangement of drivetrains in a ship?"*
  - The owner of the ship usually has a strong opinion about the machinery concept of the ship. For example, the customer can decide that the ship must have an Azipod-propulsion system for better maneuverability. Also cost of the ship construction, total-life-span costs, ecological and environmental aspects, desired fuel type, operational profile, ship size and intended use of the ship play a vital role in the design of the ship.

    Optimum loading for engines would be 85% load at service speed, including the possible shaft generator, which is in charge of the hotel load at sea. Often, however, the customer wants to define the maximum speed of the vessel, which can be considerably higher than the service speed. Propulsion engines must in this case be designed by the maximum speed. The operational time at maximum speed is often low, and it is therefore uneconomical to over-dimension the propulsion engine so that the shaft generators would be operational while operating on full load. At maximum speed the hotel load is provided by auxiliary generators. [7] [57]

- *"When is a shaft generator considered a feasible choice, and what are the design features involving such a decision?"*
  - Shaft generator is almost always a feasible option and involved in most of ship design projects. The hotel load is in these ships generated using best possible fuel efficiency provided by the main engine. Auxiliary generators are in optimum situations used only in port. Shaft generators are especially suitable for example cargo ships, since they usually have one engine coupled

to propulsion. The engine is running almost constantly since the ship is designed to sail for long periods of time. In these instances, it is important that the engine has capacity exceeding the load at service speed, in order to adjust the total engine load to optimum engine operating point with the shaft generator. [7] [57]

- *"How does the possible existence of a shaft generator affect the amount of installed electrical power on auxiliary engines?"*
    - Auxiliary generators and shaft generators are sized by the electrical balance, where the electrical load is calculated in different operational situations, gensets are sized to run at optimum load level (lowest SFC, approximately 85 % total load). Often for example RoPax ships have their highest electrical load at port at loading situations, and consequently the gensets need to be sized by this situation. Shaft generators are sized by the normal sea operation electrical load. Maneuvering situations can, however, also have significantly high electrical load due to the use of thrusters, and this needs to be into account in the total electrical capacity. [7] [57]

The inefficiencies on a ship vary substantially. If we observe the efficiency of the most efficient diesel engine in table 2, figure 6 for the best propeller in this type, and calculate that even if the power transmission in between had the efficiency of one, somewhat 60 % of all energy fed to the system in the fuel is wasted to inefficiencies. The old industry rule of thumb of two thirds of the total energy to be wasted, can be considered true.

Table 9 shows the results from tables 5 – 8 with calculated fuel savings. For the containership, the addition of a shaft generator and conversion to diesel electric seems to be inefficient. Although the dataset was poorly chosen, it seems that the efficiency of large 2-stroke diesel engine is so good that in a case like this, an electric powertrain has too many conversions causing too many sources of inefficiency.

The computation for the harbor tug shows the advantage of a diesel electric powertrain, a reduction of fuel consumption is calculated at 4 %. In this case a shaft generator does not produce significant savings. The sea lane to Inkoo from Hanko is situated at the Finnish

archipelago, where a constant speed is difficult to maintain. Therefore, the shaft generator online-time is low and variations in load are large.

The reduction of fuel consumed for operational mode 2 is somewhat what one could expect. A reduction of 2 % in the fuel consumed is quite plausible in real life. However, the operational mode 3 results for the bulk-cargo ship are somewhat surprising. A constant load-long distant journey is traditionally where the shaft generator construction has the advantage. It seems, however, that even if the additional inefficiencies accounted for, the diesel-electric propulsion might suit this kind of ship.

The computation results for the passenger ship are quite unsurprising as whole, the shaft generator in mode 2 is practically online for two short periods. The fluctuations in propulsion load means that the shaft generator is never in the synchronous speed. The Diesel-electric powertrain approx. 2.7 % of fuel, in quantity measured, just over three tons.

Table 9) Fuel savings for every ship compared to op. mode 1.

	Containership		
	Fuel used [kg]		
	op. mode 1	op. mode 2	op. mode 3
kg fuel consumed	19798	19912	21277
%-decrease to op. Mode 1	-	-0.576	-7.472

	Harbor tug		
	Fuel used[kg]		
kg fuel consumed	985	982	946
%-decrease to op. Mode 1	-	0.290	3.961

	Bulk cargo ship		
	Fuel used [kg]		
kg fuel consumed	20756	20330	19802
%-decrease to op. Mode 1	-	2.056	4.598

	Passengership		
	Fuel used [kg]		
kg fuel consumed	115080	115146	112013
%-decrease to op. Mode 1		-0.058	2.665

5 DISCUSSION AND CONCLUSIONS

The following chapter consists of the conclusions and discussion about this paper, the results and flow, reliability, validity and success of this work is described in brief. Also, recommendations for future work are given by the basis of this work.

5.1 Conclusions

Ship design and building is a complex and time-consuming project. The initial propulsive power estimate can be made with empirical methods or simulations. The customer in some cases can have a fairly good idea on what kind of a ship and ship machinery arrangement is needed for the operation of the ship, leaving the ship designer in a role of commissioner of the project. One is compelled to see that a shaft generator itself does not decrease the amount of electrical power in auxiliary generators, since hotel load and power to other consumers need to be generated in port, where the main engine is stopped. None the less, calculations suggest that a shaft generator can cut fuel consumption if planned to a vessel where this kind of arrangement is best suited, long distance-constant speed vessels. It seems that the only thing preventing a shaft generator to be installed in a ship is the available space and will of the customer that dictates whether a ship is installed with a shaft generator or not. Numerous options for a shaft generator makers and configurations exist, however, the machinery needs to be designed carefully to achieve wanted effects of the generator.

The results of the efficiency calculations are somewhat foreseeable, the shaft generator seems to decrease the fuel used in cases where the main engine rotational speed is constant for a long period of time and matches the synchronous speed of the shaft generator. A diesel-electric powertrain has its advantages, even in an unexpected load profile of bulk-cargo ship.

However efficient the electric powertrain is, it is practically always powered by a diesel engine and the power processed by the powertrain is fed to a propeller. These form the two components lowest in efficiency, so therefore a major part of total energy is none the less wasted.

5.2 Criticism

Sampling of ships and their routes was done by random choice, with a sampling number of four, the results of this paper need be considered only a as guideline. However, the

calculation model suggests in one out of four cases that a shaft generator is beneficial. A better choice of route in the containership case could had supported the shaft generator. Unfortunately, the questionnaires sent to ships and shipping companies came practically unanswered and using AIS-data as load-data decreases the validity and reliability the work.

The best outcome of this work is the calculation model, and by with the use of, the reader or anyone who is interested of the subject can self-study the problem of maritime ship optimization. The calculators can be also used for non-scientific projects and work.

Future work within the field at hand could include calculations using the same model or idea using broader sampling of ships. Obviously, since the model is based on empirical methods, the use of CFD-simulations to achieve better accuracy in the fundamental power estimate could increase the reliability of the model.

Despite everything, one needs to consider the work itself as a success. Discrete answers were found to the fundamental questions set forehand or at least to most of them. Hopefully, the calculations and model prove themselves useful to someone reding this.

REFERENCES

[1] TULLI, Finnish customs agency, "Ulkomaankaupan kuljetukset 2019," 12. 3. 2019. [Online]. Available: https://tulli.fi/-/ulkomaankaupan-kuljetukset-vuonna-2019#. [Accessed 9. 3. 2021].

[2] Ship&Bunker.com, "Maritime fuel prices Worldwide.," [Online]. Available: https://shipandbunker.com/prices#VLSFO. [Accessed 12. 3. 2021].

[3] International maritime oraganization, "Marine Environment Protection Committee (MEPC 76), 10 - 17 June 2021," [Online]. Available: https://www.imo.org/en/MediaCentre/MeetingSummaries/Pages/MEPC76meetingsummary.aspx. [Accessed 03. 11. 2021].

[4] International maritime organization, "Energy Efficiency Measures," [Online]. Available: https://www.imo.org/en/OurWork/Environment/Pages/Technical-and-Operational-Measures.aspx. [Accessed 03. 11. 2021].

[5] L. Birk, Fundamentals of Ship Hydrodynamics - Fluid Mechanics, Ship Resistance and Propulsion, West Sussex: John Wiley & Sons, 2019.

[6] P. Holtrop and G. Mennen, "An approximate power prediction method," in *Shipbuildin progress*, 1982.

[7] M. Vauhkonen, *Manager, Concept Design & Project Services. Deltamarin Ltd.* [Interview]. 22. 6. 2021.

[8] J. Carlton, Marine Propellers and Propulsion, 3 ed., Oxford: Elsevier, 2012.

[9] K. Kuiken, Diesel engines, 2 ed., Onnen: Target global energy training, 2012.

[10] M. W. C. Oosterweld. P. V. Oossanen, "Further computer-analyzed data of the Wageningen B-screw series," Netherlands Ship Model Basin, Rotterdam, 1975.

[11] E. Valtanen, Tekniikan taulukkokirja, 21 ed., Genesis kirjat Oy, 2016.

[12] Wärtsilä Oyj, "Marine engine program," [Online]. Available: https://www.wartsila.com/marine/build/engines-and-generating-sets/diesel-engines. [Accessed 24. 3. 2021].

[13] WinGD, "X92-B - leaflet," [Online]. Available: https://www.wingd.com/en/engines/engine-types/diesel/x92-b/. [Accessed 17. 4. 2021].

[14] MTU Friedrichshafen gmbh., "12V 4000 M73/M73L Datasheet," [Online]. Available: https://www.mtu-solutions.com/eu/en/products/commercial-marine-products-list.html. [Accessed 30. 3. 2021].

[15] MTU Friedrichshafen gmbh, "16V 8000 M91L Datasheet," [Online]. Available: https://www.mtu-solutions.com/eu/en/products/commercial-marine-products-list.html. [Accessed 8. 4. 2021].

[16] Caterpillar, "Commercial Propulsion Engines - 3512E marine diesel engine Datasheet," [Online]. Available: https://www.cat.com/en_US/products/new/power-systems/marine-power-systems/commercial-propulsion-engines.html?page=2. [Accessed 8. 4. 2021].

[17] Caterpillar, "Commercial Propulsion Engines - MaK M43C marine diesel engine Datasheet," [Online]. Available: https://www.cat.com/en_US/products/new/power-systems/marine-power-systems/commercial-propulsion-engines.html?page=3. [Accessed 8. 4. 2021].

[18] MAN Energy systems, ”Marine engine programme,” 2021. [Online]. Available: https://www.man-es.com/marine/products/planning-tools-and-downloads/marine-engine-programme.

[19] H. Cho, C.E. Goering, ”Engine model for mapping BSFC,” *Mathematical and computer modelling, vol.* 11, pp. 514 - 518, 1988.

[20] A. F. Molland, S. R. Turnock and D. A. Hudson, Ship Resistance and Propulsion - Practical Estimation of Ship Propulsive Power, Cambridge University Press, 2017.

[21] Wärtsilä Oyj, "Marine single input gears program," [Online]. Available: https://www.wartsila.com/marine/build/propulsors-and-gears/gears/wartsila-single-input-gear. [Accessed 8. 4. 2021].

[22] T. Z. Josef Bříoušek, "Experimental study of electric vehicle gearbox efficiency," in *MATEC Web of Conferences 234*, Liberec, Czech Republic, 2018.

[23] K. Michaelis. M. Hinterstoisser. B-R Höhn, "OPTIMIZATION OF GEARBOX EFFICIENCY," *Goriva i Maziva*, vol. 48, no. 4, pp. 441 - 480, 2009.

[24] FINNISH STANDARDS ASSOCIATION SFS , SFS-ISO 1122-1:1998 - VOCABULARY OF GEAR TERMS. PART 1: DEFINITIONS RELATED TO GEOMETRY, Helsinki, 1998.

[25] FINNISH STANDARDS ASSOCIATION SFS, SFS-ISO 21771 - GEARS. CYLINDRICAL INVOLUTE GEARS AND GEAR PAIRS. CONCEPTS AND GEOMETRY, Helsinki: FINNISH STANDARDS ASSOCIATION SFS, 2013.

[26] K. v. Dokkum, Ship knowledge - Ship design, construction and operation, 8 ed., Enkhuizen: Dokmar, 2013.

[27] Wärtsilä Oyj, "Controllable Pitch Propeller Systems -broshure," 2018. [Online]. Available: https://www.wartsila.com/marine/build/propulsors-and-gears/propellers/wartsila-controllable-pitch-propeller-systems. [Accessed 8. 4. 2021].

[28] H. Glauert, "The elements of aerofoil and airscrew theory," 2 nd. ed., Cambridge, Cambridge University Press, 1947.

[29] B. Volker, Practical ship hydrodynamics, 2nd ed., Oxford: Elsevier, 2012.

[30] B-J. Chang, H-W. Seo, K-S Min, ”Study on the contra-rotating propeller system design and full-scale performance prediction method,” *International Journal of Naval Architecture and Ocean Engineering*, nro 1, pp. 29-38, 2009.

[31] M.W.C. Osterweld, J.D. van Manen, "Model tests on contra-rotating propellers - Report nr.21444/7294/SB," Dutch ministery of defence, Gravenhage, 1969.

[32] Det Norske Veritas, "Rules for classification - Part 4 systems and components - Ch.8 Electrical installations," 7 2021. [Online]. Available: https://rules.dnv.com/ServiceDocuments/dnv/?_ga=2.261704141.1525077293.1635929878-1872003881.1617631521#!/industry/1/Maritime/1/Rules%20for%20classification:%20Ships%20(RU-SHIP). [Accessed 3. 11. 2021].

[33] Sähköinfo Oy, D1-2017 Käsikirja rakennusten sähköasennuksista, Helsinki: Sähköinfo Oy, 2017.

[34] Rolls-Royce, ”Power surge - Increasing onboard electrical power for the US Navy's DDG-51 destryers,” 2017. [Online]. Available: https://www.rolls-royce.com/media/our-stories/discover/2017/power-surge-ag9160.aspx. [Accessed 03 11. 2021].

[35] Wärtsilä Oyj, "Wärtsilä generating sets," [Online]. Available: https://www.wartsila.com/marine/build/engines-and-generating-sets/generating-sets/wartsila-gensets. [Accessed 4. 18. 2021].

[36] Caterpillar, "Caterpillar Marine Generators - MaK 34 DF marine Generator Set," [Online]. Available: https://www.cat.com/en_US/products/new/power-systems/marine-power-systems/marine-generator-sets.html. [Accessed 18. 4. 2021].

[37] MTU Friedrichshafen gmbh, "Marine and Offshore - Solution guide," [Online]. Available: https://www.mtu-solutions.com/au/en/applications/commercial-marine/system-solutions/marine-gensets.html. [Accessed 03. 11. 2021].

[38] Caterpillar marine , "Caterpillar marine generator stes," 27. 7. 2021. [Online]. Available: https://www.cat.com/en_US/products/new/power-systems/marine-power-systems/marine-generator-sets.html?page=3.

[39] Kongsberg Marine, "Marine products and systems," 2019. [Online]. Available: https://www.kongsberg.com/maritime/search/?searchTerm=Product%20catalog%202019.pdf. [Accessed 27. 7. 2021].

[40] ABB , "Marine generators-brouchure," 25. 7. 2021. [Online]. Available: https://new.abb.com/motors-generators/generators/generators-for-engines/low-voltage-generators-for-marine-applications.

[41] VEM Group, "Shipbuilding Product range," [Online]. Available: https://www.vem-group.com/en/products-services/medium-and-high-voltage/shipbuilding/product-range.html. [Accessed 20. 7. 2021.].

[42] GE Electric, "Diesel and Gas Engine Driven Generators," 25. 7. 2021. [Online]. Available: https://www.gepowerconversion.com/product-solutions/large-industrial-generators/diesel-and-gas-engine-driven-generators.

[43] GE Electric, ”Improving Fuel Efficiency and Operational Flexibility,” 25. 7. 2021. [Online]. Available: https://www.gepowerconversion.com/product-solutions/large-industrial-generators/ptopti.

[44] Cummins Generator Technologies, "NEWAGE STAMFORD AvK Alternators," [Online]. Available: https://www.stamford-avk.com/alternators. [Accessed 20. 7. 2021.].

[45] WEG S.A., "Synchronous Alternators AN10 Line," [Online]. Available: https://www.weg.net/catalog/weg/FI/en/Generation%2CTransmission-and-Distribution/Generators/Alternators-for-Generator-Sets/Naval-and-Oil-%26-Gas/Synchronous-Alternators---Naval-and-Oil-Gas/p/MKT_WEN_GENSET_NAVALOILGAS. [Accessed 20. 7. 2021.].

[46] ATB Austria Antriebstechnik AG, "ATB Products," [Online]. Available: http://www.atb-motors.com/EN/Products/ATB+Products.aspx. [Accessed 20. 7. 2021.].

[47] Brush Group, "Brush Generators and motors," 25. 7. 2021. [Online]. Available: https://www.brush.eu/generators-and-motors.

[48] Lloyd Dynamowerke gmbh, "LDW products," 25. 7. 2021. [Online]. Available: https://www.ldw.de/en/produkte.

[49] Marelli motori, "Marelli generators," 25. 7. 2021. [Online]. Available: https://www.marellimotori.com/en-GB/4936/generators.

[50] Mecc Alte S.p.a, ”Mecc Alte alternators,” 25. 7. 2021. [Online]. Available: https://www.meccalte.com/en/products/alternators/power-products-mvhv.

[51] K. Kokkila, "Azipod® M propulsion for ferries and RoPax vessels: faster, safer, cleaner," ABB Oy, 5. 6. 2019. [Online]. Available: https://new.abb.com/news/detail/24849/azipodr-m-propulsion-for-ferries-and-ropax-vessels-faster-safer-cleaner. [Accessed 18 4. 2021].

[52] ABB Oy, ”Azipod product platform selection guide,” 8. 2010. [Online]. Available: https://library.abb.com/d/9AKK105152A5238. [Accessed 07. 11. 2021].

[53] ABB Oy, ”Azipod® C gearless propulsor improves operational profitability,” [Online]. Available: https://new.abb.com/marine/generations/technology/azipod-c-gearless-propulsor-improves-operational-profitability. [Accessed 07. 11. 2021].

[54] ABB, Johanna Rosberg, ”ABB reaches 99.05% efficiency, the highest ever recorded for a synchronous motor,” 12. 7. 2017. [Online]. Available: https://www.abb-conversations.com/2017/07/abb-motor-sets-world-record-in-energy-efficiency/. [Accessed 7. 11. 2021].

[55] ABB Oy, "Industrial drive, ACS6080," [Online]. Available: https://new.abb.com/drives/medium-voltage-ac-drives/acs6080. [Accessed 03. 11. 2021].

[56] Nidec Corporation, "Silcovert FH," [Online]. Available: https://www.nidec-industrial.com/products/medium-high-voltage-drives/silcovert-fh/. [Accessed 05. 11. 2021].

[57] J. Kankare, *Design Manager, Electrical and Automation, ELOMATIC.* [Interview]. 28. 6. 2021.

[58] Kongsberg marine, "Controllable pitch propeller," [Online]. Available: https://www.kongsberg.com/maritime/products/propulsors-and-propulsion-systems/propellers/controllable-pitch-propeller/. [Accessed 03. 11. 2021].

APPENDIXES

Appendix 1 - Wageningen B polynomials

Wageningen B polynomials for propeller calculations, reproduced from [10]

$C_{s,t,u,v}{}^{T}$	Ts	Tt	Tu	Tv
0,008804960	0	0	0	0
-0,204554000	1	0	0	0
0,166351000	0	1	0	0
0,158114000	0	2	0	0
-0,147581000	2	0	1	0
-0,481497000	1	1	1	0
0,415437000	0	2	1	0
0,014404300	0	0	0	1
-0,053005400	2	0	0	1
0,014348100	0	1	0	1
0,060682600	1	1	0	1
-0,012589400	0	0	1	1
0,010968900	1	0	1	1
-0,133698000	0	3	0	0
0,006384070	0	6	0	0
-0,001327180	2	6	0	0
0,168496000	3	0	1	0
-0,050721400	0	0	2	0
0,085455900	2	0	2	0
-0,050447500	3	0	2	0
0,010465000	1	6	2	0
-0,006482720	2	6	2	0
-0,008417280	0	3	0	1
0,016842400	1	3	0	1
-0,001022960	3	3	0	1
-0,031779100	0	3	1	1
0,018604000	1	0	2	1
-0,004107980	0	2	2	1
-0,000606848	0	0	0	2
-0,004981900	1	0	0	2
0,002598300	2	0	0	2
-0,000560528	3	0	0	2
-0,001636520	1	2	0	2
-0,000328787	1	6	0	2
0,000116502	2	6	0	2
0,000690904	0	0	1	2
0,004217490	0	3	1	2
0,000056523	3	6	1	2
-0,001465640	0	3	2	2

$C_{s,t,u,v}{}^{Q}$	Qs	Qt	Qu	Qv
0,003793680	0	0	0	0
0,008865230	2	0	0	0
-0,032241000	1	1	0	0
0,003447780	0	2	0	0
-0,040881100	0	1	1	0
-0,108009000	1	1	1	0
-0,088538100	2	1	1	0
0,188561000	0	2	1	0
-0,003708710	1	0	0	1
0,005136960	0	1	0	1
0,020944900	1	1	0	1
0,004743190	2	1	0	1
-0,007234080	2	0	1	1
0,004383880	1	1	1	1
-0,026940300	0	2	1	1
0,055808200	3	0	1	0
0,016188600	0	3	1	0
0,003180860	1	3	1	0
0,015896000	0	0	2	0
0,047172900	1	0	2	0
0,019628300	3	0	2	0
-0,050278200	0	1	2	0
-0,030055000	3	1	2	0
0,041712200	2	2	2	0
-0,039772200	0	3	2	0
-0,003500240	0	6	2	0
-0,010685400	3	0	0	1
0,001109030	3	3	0	1
-0,000313912	0	6	0	1
0,003598500	3	0	1	1
-0,001421210	0	6	1	1
-0,003836370	1	0	2	1
0,012680300	0	2	2	1
-0,003182780	2	3	2	1
0,003342680	0	6	2	1
-0,001834910	1	1	0	2
0,000112451	3	2	0	2
-0,000029723	3	6	0	2
0,000269551	1	0	1	2
0,000832650	2	0	1	2
0,001553340	0	2	1	2
0,000302683	0	6	1	2
-0,000184300	0	0	2	2
-0,000425399	0	3	2	2
0,000086924	3	3	2	2
-0,000465900	0	6	2	2
0,000055419	1	6	2	2

Appendix 2 - MATLAB propeller calculator

MATLAB- code for propeller calculation

```
% Wageningen.mlx - Propeller calculator
% initial parameters
% inport polynomials as column vectors to corresponding variables


Po = ;          % static pressure at shaft centerline in kg/m^2
Pv = ;          % vapour pressure of water in kg/m^2
Cb = ;          % block coefficient of the vessel
roo = 1025;        % water density in kg/m3
K = ;           % constant,
               % 0.0 for fast two shaft vessels,
               % 0.1 for other two shaft vessels and
               % 0.2 for one shaft vessels


% Propeller diameter or shaft rpm calulation, select either D or RPM to
unknown by setting = 0
% Propeller operating point calculation by no unknown parameters
D = ;           % propeller diameter in m
RPM = ;          % Shaft RPM
T = ;           % desired propeller thurst in N for min_area calculation
bl = ;          % number of blades on the propeller
Vs = ;          % Vessel design speed in m/s
PD_prop = ;                          % pitch/diameter ratio, if known. CPP =
0.
w_s = ;          % wake fraction of the hull, if unknown = 0




% Minimum blade area ratio based on cavitation, Keller formula
min_area = (((1.3 + 0.3*bl)*(T/9.81))/((Po-Pv)*(D^2))+K);


area = 0.8;       % selected blade expanded area ratio, range 0.3 - 1.05. if
unknown, select = min_area


%speed of advance using Taylor's method or known wake fraction
if w_s == 0
  Va = (1-(0.5*Cb-0.05))*Vs;
else
  Va = Vs*(1-w_s);
end


J = (0.0005:0.0005:1.5);    % Advance ratio range
PD = (0.5:0.1:1.4);   % Pitch/Diameter range, 0.1 interval
```

```
lT = length(CstuvT);  % number of thrust polynominals
lQ = length(CstuvQ);  % number of torque polynominals
l = length(J);     % number of datapoints
v = 1;
b = 1;
d = 1;
x = 0;
K_Tcpp = [];
K_Qcpp = [];
K_T = [];
K_Q = [];
n0 = [];
nJ = [];
```

```
% Calculation of thrust coefficients per P/D
for g = 1:1:length(PD)
  for c = 1:1:length(J)
    for a = 1:1:lT
      x = x +
(CstuvT(b)*((J(d)^(Ts(b))))*(PD(v)^(Tt(b)))*(area^(Tu(b)))*(bl^(Tv(b))));
      b = b + 1;
    end
      if x < 0
        x = 0;
      end
    K_Tcpp(d,v) = x;
    x = 0;
    b = 1;
    d = d + 1;
  end
  d = 1;
  v = v + 1;
end
v = 1;
plot(J,K_Tcpp(1:l,1),J,K_Tcpp(1:l,2),J,K_Tcpp(1:l,3),J,K_Tcpp(1:l,4),J,K_Tcp
p(1:l,5),J,K_Tcpp(1:l,6),J,K_Tcpp(1:l,7),J,K_Tcpp(1:l,8),J,K_Tcpp(1:l,9),J,K
_Tcpp(1:l,10))
ylim([0 1])
legend('P/D = 0.5','P/D = 0.6','P/D = 0.7','P/D = 0.8','P/D = 0.9','P/D =
1.0','P/D = 1.1','P/D = 1.2','P/D = 1.3','P/D = 1.4')
title(['Wageningen B-series, ',num2str(bl), ' blades, Ae/Ao=
',num2str(area)])
xlabel('Advance ratio (J)')
ylabel('Thrust coefficient')
```

```
% Calculation of torque coefficients per P/D
for g = 1:1:length(PD)
  for c = 1:1:length(J)
    for a = 1:1:lQ
```

```
      x = x +
(CstuvQ(b)*((J(d)^(Qs(b))))*(PD(v)^(Qt(b)))*(area^(Qu(b)))*(bl^(Qv(b))));
      b = b + 1;
    end
    if x < 0
      x = 0;
    end
    if K_Tcpp(d,v) == 0
      x = 0;
    end
    K_Qcpp(d,v) = x;
    x = 0;
    b = 1;
    d = d + 1;
  end
  d = 1;
  v = v + 1;
end
v = 1;
plot(J,K_Qcpp(1:l,1),J,K_Qcpp(1:l,2),J,K_Qcpp(1:l,3),J,K_Qcpp(1:l,4),J,K_Qcp
p(1:l,5),J,K_Qcpp(1:l,6),J,K_Qcpp(1:l,7),J,K_Qcpp(1:l,8),J,K_Qcpp(1:l,9),J,K
_Qcpp(1:l,10))
ylim([0 0.3])
legend('P/D = 0.5','P/D = 0.6','P/D = 0.7','P/D = 0.8','P/D = 0.9','P/D =
1.0','P/D = 1.1','P/D = 1.2','P/D = 1.3','P/D = 1.4')
title(['Wageningen B-series, ',num2str(bl), ' blades, Ae/Ao=
',num2str(area)])
xlabel('Advance ratio (J)')
ylabel('Torque coefficient')
```

```
% Calculation of propeller efficency per P/D
for h = 1:1:length(PD)
  for j = 1:1:l
    if K_Qcpp(v,b) == 0
      n0(v,b) = 0;
    else
      n0(v,b) = (J(v)/(2*pi))*(K_Tcpp(v,b)/K_Qcpp(v,b));
    end
    v = v + 1;
  end
  v = 1;
  b = b + 1;
end
v = 1;
b = 1;
plot(J,n0(1:l,1),J,n0(1:l,2),J,n0(1:l,3),J,n0(1:l,4),J,n0(1:l,5),J,n0(1:l,6)
,J,n0(1:l,7),J,n0(1:l,8),J,n0(1:l,9),J,n0(1:l,10))
ylim([0 1])
legend('P/D = 0.5','P/D = 0.6','P/D = 0.7','P/D = 0.8','P/D = 0.9','P/D =
1.0','P/D = 1.1','P/D = 1.2','P/D = 1.3','P/D = 1.4')
```

```
title(['Wageningen B-series, ',num2str(bl), ' blades, Ae/Ao=
',num2str(area)])
xlabel('Advance ratio (J)')
ylabel('Efficiency')


% Calculation efficiency on CPP-prop. and optimum design parameters
if PD_prop == 0
  dydxK_T = -(K_Tcpp(1,1))/(max(J));
  dydxK_Q =-(K_Qcpp(1,1))/(max(J));
  for h = 1:1:length(J)
    if n0(v,:) == 0
      nJ(v) = 0;
    else
      nJ(v) = max(n0(v,:))-0.03;
    end


    K_T(v) = K_Tcpp(1,1)+ dydxK_T*J(v);
    K_Q(v) = K_Qcpp(1,1)+ dydxK_Q*J(v);
    v = v +1;
  end
  x = 1;
  v = 1;
  plot(J,K_T,J,K_Q,J,nJ)
  ylim([0 1])
  legend('Thrust coeff.','Torque coeff.','Efficiency - CPP')
  title(['Wageningen B-series, ',num2str(bl), ' blades, Ae/Ao=
',num2str(area),' - CPP-propeller'])
  xlabel('Advance ratio (J)')
  ylabel('Efficiency')
end


% Calculations for specific P/D-ratio
if PD_prop ~= 0
  for c = 1:1:length(J)
    for a = 1:1:lT
      x = x +
(CstuvT(b)*((J(d)^(Ts(b))))*(PD_prop^(Tt(b)))*(area^(Tu(b)))*(bl^(Tv(b))));
      b = b + 1;
    end
      if x < 0
        x = 0;
      end
    K_T(d) = x;
    x = 0;
    b = 1;
    d = d + 1;
  end
  d = 1;
```

```
  for c = 1:1:length(J)
    for a = 1:1:lQ
      x = x +
(CstuvQ(b)*((J(d)^(Qs(b))))*(PD_prop^(Qt(b)))*(area^(Qu(b)))*(bl^(Qv(b))));
      b = b + 1;
    end
    if x < 0
      x = 0;
    end
    if K_T(d) == 0
      x = 0;
    end
    K_Q(d) = x;
    x = 0;
    b = 1;
    d = d + 1;
  end
  d = 1;

  for j = 1:1:l
    nJ(v) = (J(v)/(2*pi))*(K_T(v)/K_Q(v));
    v = v + 1;
  end
  v = 1;
  plot(J,K_T,J,K_Q,J,nJ)
  ylim([0 1])
  legend('Thrust coeff.','Torque coeff.','Efficiency')
  title(['Wageningen B-series, ',num2str(bl), ' blades, Ae/Ao=
',num2str(area),' - FPP-propeller, P/D= ',num2str(PD_prop)])
  xlabel('Advance ratio (J)')
  ylabel('Efficiency, kQ, kT')
end


for j = 1:1:l
  if x < nJ(v)
    x = nJ(v);
    b = j;
  end
  v = v + 1;
end
v = 1;


% Design parameter calculations if shaft RPM is unknown
if RPM == 0
  J_opt = J(b)
  RPM_opt = (Va/(J_opt*D))*60
  Torque = K_Q(b)*roo*((RPM_opt/60)^2)*(D^5)
  Thrust = K_T(b)*roo*((RPM_opt/60)^2)*(D^4)
```

```
  Shaft_power = Torque*2*pi*(RPM_opt/60)
  n_opt = nJ(b)
end


% Design parameter calculations if diameter is unknown
if D == 0
  J_opt = J(b)
  D_opt = (Va/(J_opt*(RPM/60)))
  kT_opt = K_T(b)
  kQ_opt = K_Q(b)
  Torque = K_Q(b)*roo*((RPM/60)^2)*(D_opt^5)
  Thrust = K_T(b)*roo*((RPM/60)^2)*(D_opt^4)
  Shaft_power = Torque*2*pi*(RPM/60)
  n_opt = nJ(b)
end


% Operating point tracking if diameter and shaft RPM are known
if D ~= 0 && RPM ~= 0
  J_op = Va/(D*(RPM/60))
  b = find(abs(J-J_op) < 0.00025);
  kT_op = K_T(b)
  kQ_op = K_Q(b)
  Torque = K_Q(b)*roo*((RPM/60)^2)*(D^5)
  Thrust = K_T(b)*roo*((RPM/60)^2)*(D^4)
  Shaft_power = Torque*2*pi*(RPM/60)
  n_op = nJ(b)
end
v = 1;
b = 1;
x = 0;


% End of file
```

Appendix 3 - Ship resistance and power estimation calculator based on Holtrop-Mennen- and ITTC78-methods

```
% HoltropMennen.mlx
% initial parameters
roo = 1025;       % water density
myy = 0.0000011892;   % water kinematic viscosity



% required parameters
V_s = ;         % ship speed in m/s, import data as a vector
L_wl = ;       % waterline length
B = ;         % molded beam
T_a = ;       % molded draft at aft perpendicular
T_f = ;       % molded draft at forward perpendicular
V = ;       % molded volumetric displacement
C_p = ;      % prismatic coefficient
C_wp = ;       % waterplane area coefficient
A_v = ;       % area of ship and cargo above waterline
A_bt = ;       % transverse area of bulbous bow
h_b = ;       % height of center of A_bt above basis, has to be smaller than
0.6*T_f
shafts = ;       % number of shafts, 1 or 2
D = ;         % propeller diameter
AeAo = ;       % propeller expanded area ratio
PD = ;         % propeller pitch/diameter ratio
C_stern = ;      % stern shape parameter
              % pram with gondola = -25
              % V-shaped sections = -10
              % normal sections = 0
              % U-shaped sections = +10


% optional parameters, if unknown set to zero
A_t = 0;        % immersed transom area
T = 0;         % molded mean draft
S = 0;         % hull wetted surface area
i_e = 0;        % half angle of waterline entrance
d_th = 0;        % diameter of bow thruster tunnel
L_cb = 0;        % longitudinal center of buoyancy in meters from midship
(L_wl/2), negative in aft direction
C_b = 0.0;        % block coefficient
C_m = 0;        % midship section coefficient
k_s = 0;        % hull rouhness


% Appendage k2_i value and area listing, list values in vectors "S_app" and
% "k2" to their corresponding places according table 1
```

```
S_app = [0];      % Surface areas of appendages
k2 = [0];      % k2_i value of each appendage


T_req = [];
C_s = [];
V_a = [];
RPS = [];
J_sp = [];
Kt_sp = [];
Kq_sp = [];
no_sp = [];
Prop_torque = [];
Del_power = [];
```

Appendage (Table 1)	$k2i$ value
rudder behind skeg	0.2 - 0.5
rudder behind stern	0.5
twin screw rudder (slender)	1.5
twin screw rudder (thick)	2.5
shaft brackets	2.0 - 4.0
skeg	0.5 - 1.0
strut bossing	2.0 - 3.0
hull bossing	1.0
exposed shafts (angle with buttocks about 10 degrees)	1.0
(angle with buttocks about 20 degrees)	4.0
stabilizer fins	1.8
dome	1.7
bilge keels	0.4

```
n = 1;
for c = 1:1:length(V_s)
  if V_s == 0
    V_s = 0.000000000000000000001
  end
  % unknown parameter estimation/calculation
  if T == 0
    T = 0.5*(T_a+T_f);
  end
  if C_b == 0
    C_b = V/(B*T*L_wl);
  end
  Fr = V_s(n)/sqrt(9.81*L_wl);

  if L_cb == 0
    l_cb= -(0.44*Fr-0.094)*100;
  else
    l_cb = -(L_cb/L_wl)*100;
  end
```

```
  if C_m == 0
    C_m = abs(1/(1+(1-C_b)^3.5));
  end

  if S == 0
    c_23 = 0.453+(0.4425*C_b)-(0.2862*(C_m))-(0.003467*(B/T))+(0.3696*C_wp);
    S=
L_wl*((2*T)+B)*sqrt(C_m)*((0.615989*c_23)+(0.111439*(C_m^3))+(0.000571111*C_
stern)+(0.245357*(c_23/C_m)))+(3.345538*A_t)+(A_bt/C_b)*(1.4660538+(0.583949
7/C_m));
  end


  L_r = L_wl*((1-C_p+0.06*C_p*l_cb)/((4*C_p)-1));
  if i_e == 0
    a = -((((L_wl/B)^0.80856))*((1-C_wp)^0.30484)*((1-C_p-
(0.0225*l_cb))^0.6367)*((L_r/B)^0.34574)*(((100*V)/(L_wl^3))^0.16302));
    i_e = 1+89*exp(a);
  end
```

```
  % frictional resistance and form factor
  Re = (V_s(n)*L_wl)/myy;
  c_14 = 1+0.011*C_stern;
  k = abs(-
0.07+(0.487118*c_14)*(((B/L_wl)^1.06806)*((T/L_wl)^0.46106)*((L_wl/L_r)^0.12
1563)*(((L_wl^3)/V)^0.36486)*((1-C_p)^(-0.604247))));
  C_f = 0.075/((log10(Re)-2)^2);
  R_f = 0.5*roo*(V_s(n)^2)*S*C_f;
```

```
  % appendage resistance
  C_dth = 0.007;   % The drag coefficient CDTH for the thruster tunnel
takes values between 0.003 and
            % 0.012. The smaller values are for thrusters which are in the
cylindrical part of the
            % bulbous bow, i.e. the rim of the opening is fairly parallel to
the midship plane.
  z = 1;
  y = 0;
  S_app_tot = 0;
  for x = 1:1:length(k2)
    y = y + ((1+k2(z))*S_app(z));
    S_app_tot = S_app_tot + S_app(z);
    z = z + 1;
  end
  if S_app_tot == 0
    k2_tot = 0;
  else
    k2_tot = y/S_app_tot;
```

```
  end
  R_th = roo*(V_s(n)^2)*pi*(d_th^2)*C_dth;
  R_app = 0.5*roo*(V_s(n)^2)*k2_tot*C_f*S_app_tot+R_th;
  z = 1;
  y = 0;
```

```
  % wave resistance and wave resistance coefficients
  if B/L_wl <= 0.11
    c7 = 0.229577*((B/L_wl)^(1/3));
  elseif (0.11 < B/L_wl) && (B/L_wl <= 0.25)
    c7 = B/L_wl;
  else
    c7 = 0.5-0.0625*(L_wl/B);
  end
  c1 = abs(2223105*(c7^3.78613)*((T/B)^1.07961)*((90-i_e)^-1.37565));
  c3 = 0.56*(((A_bt)^1.5)/((B*T*(0.31*sqrt(A_bt)+T_f-h_b))));
  c2 = abs(exp(-1.89*sqrt(c3)));
  c5 = 1-(0.8*(A_t/(B*T*C_m)));
  if (L_wl^3)/V <= 512
    c15 = -1.69385;
  elseif (512 < (L_wl^3)/V) && ((L_wl^3)/V <= 1726.91)
    c15 = -1.69385+ ((L_wl/(V^(1/3))-8)/2.36);
  else
    c15 = 0;
  end
  if C_p <= 0.8
    c16 = (8.07981*C_p)-(13.8673*(C_p^2))+(6.984388*(C_p^3));
  else
    c16 = 1.73014-(0.70667*C_p);
  end
  d = -0.9;
  if L_wl/B <= 12
    lambda = (1.446*C_p)-(0.03*(L_wl/B));
  else
    lambda = (1.446*C_p)-0.36;
  end
  m1 = (0.0140407*(L_wl/T))-(1.75254*((V^(1/3))/L_wl))-(4.79323*(B/L_wl))-
c16;
  m4 = 0.4*c15*exp(-0.034*(Fr^-3.29));
  c17 = (6919.3*(C_m^(-1.3346)))*((V/(L_wl^3))^2.00977)*(((L_wl/B)-
2)^1.40692);
  m3 = -7.2035*((B/L_wl)^0.326869)*((T/B)^0.605375);

  if V_s(n) == 0
    R_w = 0;
  elseif Fr <= 0.4
    R_w = abs(c1*c2*c5*roo*9.81*V*exp(m1*(Fr^d)+m4*cos(lambda*(Fr^(-2)))));
  elseif (0.4 < Fr) && (Fr <= 0.55)
    m4_04 = 0.4*c15*exp(-0-034*(0.4^-3.29));
    m4_55 = 0.4*c15*exp(-0-034*(0.55^-3.29));
```

```
    R_wa04 = c1*c2*c5*roo*9.81*V*exp(m1*(0.4^d)+m4_04*cos(lambda*(Fr^(-
2))));
    R_wb55 = c17*c2*c5*roo*9.81*V*exp(m3*(0.55^d)+m4_55*cos(lambda*(Fr^(-
2))));
    R_w = abs(R_wa04 + (((20*Fr-8)/3)*(R_wb55-R_wa04)));
  else
    R_w = abs(c17*c2*c5*roo*9.81*V*exp(m3*(Fr^d)+(m4*cos(lambda*(Fr^(-
2))))));
  end
```

```
  % bulbous bow resistance
  h_f = C_p*C_m*((B*T)/L_wl)*(136-(316.3*Fr))*(Fr^3);
  h_w = ((i_e*(V_s(n)^2))/(400*9.81));
  if h_f <= (-0.01*L_wl)
    h_f = -0.01*L_wl;
  end
  if h_w > (0.01*L_wl)
    h_w = 0.01*L_wl;
  end
  Fr_i = abs(V_s(n)/sqrt(9.81*(T_f-h_b-
(0.25*sqrt(A_bt)))+(0.15*(V_s(n)^2))));
  P_b = 0.56*(sqrt(A_bt)/((T_f-(1.5*h_b))));
  R_b = 0.11*roo*9.81*(sqrt(A_bt)^3)*(((Fr_i)^3)/(1+(Fr_i^2)))*exp(-
3.0*(P_b^(-2)));
```

```
  % transom resistance
  if A_t < 0
    Fr_t = V_s(n)/sqrt((2*9.81*A_t)/(B+B*C_wp));
  else
    Fr_t = 0;
  end
  if Fr_t < 5
    c6 = 0.2*(1-(0.2*Fr_t));
  else
    c6 = 0;
  end
  R_tr = 0.5*roo*(V_s(n)^2)*A_t*c6;
```

```
  % model correlation resistance
  if T_f/L_wl <= 0.04
    c4 = T_f/L_wl;
  else
    c4 = 0.04;
  end
  C_a = (0.006*((L_wl+100)^(-0.16)))-
0.00205+(0.003*sqrt(L_wl/7.5)*(C_b^4)*c2*(0.04-c4));
  if k_s <= 0.000015
    dC_a = 0;
  else
```

```
    dC_a = (0.105*(k_s^(1/3))-0.005579)/(L_wl^(1/3));
  end
  R_a = 0.5*roo*(V_s(n)^2)*(C_a+dC_a)*(S+S_app_tot);


  % air resistance
  R_aa = 0.5*1.225*(V_s(n)^2)*0.8*A_v;


  % total resistance
  R_t = abs((1+k)*R_f+R_app+R_a+R_w+R_b+R_tr+R_aa);


  %Hull-propeller interaction
  b = 1;
  if B/T_a <= 5
    c8 = (S/(L_wl*D))*(B/T_a);
  else
    c8 = (S*(7*(B/T_a)-25))/(L_wl*D*((B/T_a)-3));
  end
  if c8 <= 28
    c9 = c8;
  else
    c9 = 32-(16/(c8-24));
  end
  if T_a/D <= 2
    c11 = T_a/D;
  else
    c11 = (0.0833333*((T_a)^3))+1.3333;
  end
  if C_p <= 0.7
    c19 = ((0.12997)/(0.95-C_b))-((0.11056)/(0.95-C_p));
  else
    c19 = ((0.18567)/(1.3571*C_m))-0.71276+(0.38648*C_p);
  end
  c20 = 1+(0.015*C_stern);
  C_p1 = 1.45*C_p-0.315-0.0225*l_cb;
  if V_s(n) == 0
    C_v = 0;
  else
  C_v = (((1+k)*R_f)+R_app+R_a)/(0.5*roo*9.81*(V_s(n)^2)*(S+S_app_tot));
  end
  if shafts == 1
    wake_fraction =
abs((c9*c20*C_v*(L_wl/T_a)*(0.050776+0.93405*((c11*C_v)/(1-
C_p1))))+(0.27915*c20*sqrt(B/(L_wl*(1-C_p1))))+c19*c20);
    thrust_deduction_factor =
((0.25014*((B/L_wl)^0.28956)*((sqrt(B*T)/D)^0.2624))/((1-
C_p+0.0225*l_cb)^0.01762))+0.0015*C_stern;
    rel_rotative_eff = 0.9922-0.05908*AeAo+0.07424*(C_p-0.0225*l_cb);
  elseif shafts == 2
    wake_fraction = 0.3095*C_b+10*C_v*C_b-0.23*(D/(sqrt(B*T)));
```

```
    thrust_deduction_factor = 0.325*C_b-0.1885*(D/sqrt(B*T));
    rel_rotative_eff = 0.9737+0.111*(C_p-0.0225*l_cb)-0.06325*(PD);
  end
  T_req(n) = R_t/((1-thrust_deduction_factor)*shafts);
  V_a(n) = V_s(n)*(1-wake_fraction);
  C_s(n) = T_req(n)/(roo*(D^2)*(V_a(n)^2));
  b = 1;
  for e = 1:1:length(J)
    CSJ(n) = C_s(n)*(J(b)^2);
    if CSJ(n) < K_T(b)
      b = b + 1;
    end
  end
  n_hull = (1-thrust_deduction_factor)/(1-wake_fraction);
  J_sp(n) = J(b);
  Kt_sp(n) = K_T(b);
  Kq_sp(n) = K_Q(b)/rel_rotative_eff;     % Torque in conditions behind the
hull
  no_sp(n) = nJ(b)*rel_rotative_eff*n_hull;     % efficiency in conditions
behind the hull
  RPS(n) = V_a(n)/(J_sp(n)*D);
  Prop_torque(n) = roo*(RPS(n)^2)*(D^5)*Kq_sp(n);
  Del_power(n) = 2*pi*RPS(n)*Prop_torque(n)*shafts;


  n = n + 1;


end
plot(1:1:length(V_s),Del_power/1000000, 1:1:length(V_s), hotel_load/1000000,
1:1:length(V_s),V_s)
%,1:1:length(V_s), V_s
legend('Propulsive power','Hotel load', 'Speed')
%title('Ship propulsive power and hotel load in MW')
ylabel('Load in MW, Speed in m/s')
xlabel('datapoint')


% end of file
```

Appendix 4 – Fuel consumption calculator

```
%Fuelconsumption.mlx
op_mode = ;           % ship operating mode, 1 = aux engines + M. engine. 2
= shaft generator enabled. 3 = electric propulsion.
P_AE = ;            % Single auxiliary engine peak power in W
Best_ME_SFC = ;         % Main engine best Sfc-value
Best_AE_SFC = ;         % Auxlillary engine best SFC-value
ME_SFC = [];
AE_Load = [];
SG_load = [];
n_drivetrain = ;         % drivetrain efficincy
fuel_propulsion = 0;
fuel_hotel = 0;
Datapoint_len = 1/12;      % timelenghth of datapoint in AIS and hotel load
data in hours
hotel_load1 = hotel_load;    % additional copy of hotel_load data for
multiple calculations


max_prop_T = max(Prop_torque);
ME_rps = RPS/(max(RPS));
ME_rps_round = round(ME_rps,1)*10;
q = 1;
for x = 1:1:length(hotel_load)
  T_hotel(q) = hotel_load(q)/(2*pi*RPS(q));
  q = q + 1;
end
q = 1;
z = 1;
for x = 1:1:length(V_s)
  if op_mode == 2
    if ME_rps_round(z) == 7 && ME_torque(z)+(T_hotel(z)) < max_prop_T
      ME_torque(z) = T_hotel(z) + Prop_torque(z);
      ME_torque_PU(z) = ME_torque(z)/max_prop_T;
      ME_torque_round(z) = round(ME_torque_PU(z),1)*10;
      SG_load(z) = hotel_load1(z);
      hotel_load1(z) = 0;
    else
      if RPS(z) == 0
        ME_torque(z) = 0;
      else
      ME_torque(z) = Prop_torque(z);
      ME_torque_PU(z) = ME_torque(z)/max_prop_T;
      ME_torque_round(z) = round(ME_torque_PU(z),1)*10;
      SG_load(z) = 0;
      end
    end
  elseif op_mode == 3
    hotel_load1(z) = hotel_load1(z) + (Del_power(z)/n_drivetrain);
    ME_torque(z) = 0;
```

```
    SG_load(z) = 0;
  else
    if RPS(z) == 0
      ME_torque(z) = 0;
    else
      ME_torque(z) = Prop_torque(z);
    end
    ME_torque_PU(z) = ME_torque(z)/max_prop_T;
    ME_torque_round(z) = round(ME_torque_PU(z),1)*10;
    SG_load(z) = 0;
  end



  if op_mode ~= 3
    if ME_torque_round(z) == 0 || isnan(ME_torque_round(z))
      ME_torque_round(z) = 1;
    end
    if ME_rps_round(z) == 0 || isnan(ME_torque_round(z))
      ME_rps_round(z) = 1;
    end
    ME_SFC(z) = SFCmap(ME_rps_round(z),ME_torque_round(z))*Best_ME_SFC;
    ME_power(z) = (ME_torque(z)*2*pi*RPS(z))/n_drivetrain;
    fuel_propulsion = fuel_propulsion +
(ME_SFC(z)/1000)*ME_power(z)*Datapoint_len*shafts;
  end
  if hotel_load1(z) == 0
    No_AE(z) = 0;
    AE_Load(z) = 0;
    AE_Torque(z) = 0;
  else
    No_AE(z) = fix((hotel_load1(z)/P_AE)+0.2)+1;
    AE_Load(z) = (hotel_load1(z)/No_AE(z))/(P_AE);
    AE_Torque(z) = round(AE_Load(z),1)*10;
    if AE_Torque(z) == 0
      AE_Torque(z) = 1;
    end
  end

  if AE_Torque(z) == 0
    AE_SFC(z) = 0;
  else
    AE_SFC(z) = SFCmap(7,AE_Torque(z))*Best_AE_SFC;
  end
  fuel_generator = fuel_generator +
(AE_SFC(z)/1000)*AE_Load(z)*P_AE*No_AE(z)*Datapoint_len;
  z = z +1;
end
z = 1;
if op_mode == 2
```

```
plot(1:1:length(V_s),hotel_load1/1000000,1:1:length(V_s),No_AE,1:1:length(V_
s),ME_power*1/1000000)
  legend('Aux.gen. Load in MW','Number of Aux. engines online','Main engine
load in MW')
elseif op_mode == 3
  plot(1:1:length(V_s),hotel_load1/1000000,1:1:length(V_s),No_AE)
  legend('Total Generator load in MW','Number of Generators online')
  %ylim([0 (max(hotel_load1)/1000000)+1])
else

plot(1:1:length(V_s),hotel_load1/1000000,1:1:length(V_s),No_AE,1:1:length(V_
s),ME_power*1/1000000)
  legend('Hotel Load in MW','Number of Aux. engines online','Main engine
load in MW')
end



%End of file
```